

Quark elastic scattering as a source of high-transverse-momentum mesons*

R. D. Field and R. P. Feynman

California Institute of Technology, Pasadena, California 91125

(Received 20 October 1976)

We investigate the consequences of the assumption that the high-transverse-momentum particles seen in hadron-hadron collisions are produced by a single, hard, large-angle elastic scattering of quarks, one from the target and one from the beam. The fast outgoing quarks are assumed to fragment into a cascade jet of hadrons. The distributions of quarks in the incoming hadrons are determined from lepton-hadron inelastic scattering data, together with certain theoretical constraints such as sum rules, etc. The manner in which quarks cascade into hadrons is determined from particle distributions seen in lepton-hadron and lepton-lepton collisions supplemented by theoretical arguments. The quark elastic scattering cross section is parametrized in a purely phenomenological way and the choice $d\sigma/d\hat{t} = 2.3 \times 10^6 / (-\hat{s}\hat{t}^3) \mu b \text{ GeV}^6$ gives a reasonable fit to all the data for hadron + hadron \rightarrow meson + anything for $p_{\perp} \gtrsim 2 \text{ GeV}/c$. Many predictions do not depend sensitively on the exact form for $d\sigma/d\hat{t}$ and therefore test our basic assumption. The data examined include single-particle production in $p\bar{p}$ collisions at various energies and angles. Particle ratios (π^+, π^-, K^+, K^- , and η) are predicted and discussed. In addition, the ratio of production of π^0 's by beams of π^+ and protons on a proton target is explained. With this model we have found no serious inconsistency with data, but several predictions for charge ratios and beam ratios at other angles are presented that have yet to be tested experimentally.

I. INTRODUCTION

When hadrons collide at high energy most of the energy appears in many particles moving in the directions of the original momenta with only a small transverse momentum $\langle p_{\perp} \rangle \approx 0.35 \text{ GeV}$. There are, however, a few hadrons of unusually high transverse momenta. When this was first discovered it was hoped that they arose from an intimate hard collision between the constituent partons of the colliding hadrons. Their study could therefore lead to a deeper understanding of the short-distance behavior of the fundamental strong forces. However, this plan has so far been frustrated by two features. First, the expectation from all field theories (and there is no other consistent relativistic formulation of quantum theory) suggests that the cross sections with all momenta scaled in the same proportion should fall off with p_{\perp} nearly as p_{\perp}^{-4} (with possible logarithmic modifications), whereas experimentally the behavior is closer to p_{\perp}^{-3} .

Because of this, many theorists have suggested that we are not yet observing the fundamental interaction between partons, but some other more complex mechanism—and only at much larger energies will the expected p_{\perp}^{-4} appear (after the other mechanism, falling as p_{\perp}^{-3} , has fallen away). There is no consensus on what this other mechanism, which is operating in the present experimental region, might be; very many theories are available.

The second frustrating feature is that the observed large- p_{\perp} particles need not be particles

which are originally directly driven out, but may be the result of a disintegration or fragmentation of these originals. Interpretation of the data then needs considerable theoretical analysis requiring many assumptions of mechanism and decay functions. This makes it difficult, in any comparison to experiment, to judge from a fit whether the mechanism proposed by the theory is verified, or merely that the many possible unknown functions have been cleverly adjusted to fit.

We have no easy solution to these difficulties. In fact, after trying phenomenologically to test and distinguish some of the various models we have become unusually sensitive to these frustrations. We feel the only way out is a long hard job. One must take some one model and test it against everything experimentally available at the same time. Then if it succeeds, or can be adjusted to succeed so far, make as definite predictions as possible for experiments soon to come—indicating those which, if not fulfilled, will prove the model wrong. Only in that way can models be eliminated and progress made. In this paper we shall begin this work starting with one particular model.

The model we shall choose is not a popular one, so that we will not duplicate too much of the work of others who are similarly analyzing various models (e.g., constituent-interchange model, multiperipheral-type models, etc.). We shall assume that the high- p_{\perp} particles arise from direct hard collisions between constituent quarks in the incoming particles, and in a fundamental quark_a + quark_b \rightarrow quark_a + quark_b elastic collision the primary outgoing high- p_{\perp} particles are quarks

(in fact, of the same flavor as the quarks that came in), which fragment or cascade down into several hadrons.¹ This is illustrated in Fig. 1. We disregard the theoretical argument that this elastic cross section [which we write as $d\hat{\sigma}/d\hat{s}(\hat{s}, \hat{t})$, where \hat{s} and \hat{t} are the s, t invariants for the quark collision] must vary as $\hat{s}^{-2}f(\hat{t}/\hat{s})$ and, instead, leave it as an unknown function to be determined empirically by the data. It will vary more like $\hat{s}^{-N}f(\hat{t}/\hat{s})$ with N about 4.

We shall need the distributions $G_{h \rightarrow q}(x)$ of quarks q in the initial hadrons; for protons and neutrons this is given to a large extent by deep-inelastic $e p$ (or μp) scattering data. Also, we shall need to know what the chances, $D_q^h(z)$, are that a quark q going out at large momentum disintegrates into various kinds of hadrons, h , with a fraction z of

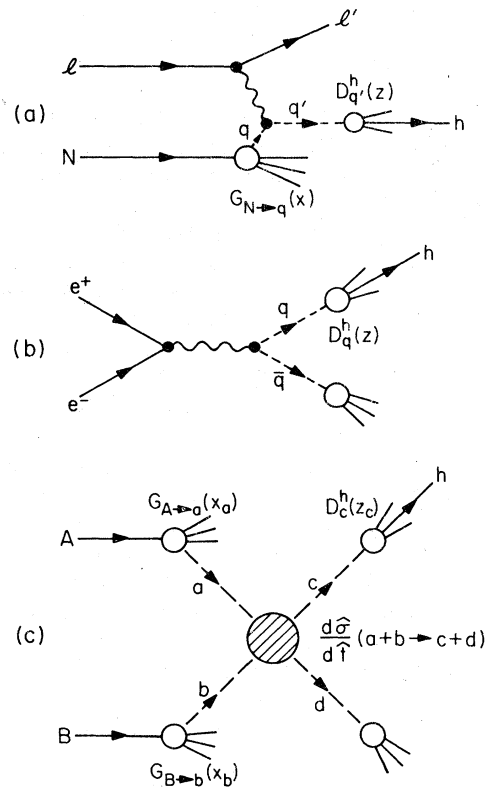


FIG. 1. (a) Quark-parton-model mechanism for single-hadron production in lepton-hadron processes. (b) Quark-parton-model mechanism for single-hadron production in e^+e^- annihilation. (c) Illustration of the common underlying structure of constituent or "hard-scattering" models for hadron-hadron collisions. The large-transverse-momentum reaction $A + B \rightarrow h + X$ is assumed to occur as a result of a single large-angle scattering of constituents $a + b \rightarrow c + d$, followed in general by the decay or fragmentation of c into the observed particle h . We further hypothesize that the dominant basic subprocess is the elastic scattering of quarks ($q_a + q_b \rightarrow q'_a + q'_b$).

the original momentum of the quark. This is given, in principle, by the hadrons produced by the recoil quarks in deep-inelastic neutrino proton scattering. Unfortunately, in both cases the data are incomplete and must be supplemented by theoretical arguments that require much discussion. This first paper deals primarily with these functions $G_{h \rightarrow q}(x)$ and $D_q^h(z)$ and with the behavior of outgoing particle and incoming beam ratios for large- p_\perp single-particle production. We examine various forms for $d\hat{\sigma}/d\hat{t}$ and make predictions that are insensitive to its detailed form. Since the behavior of $G_{h \rightarrow q}(x)$ and $D_q^h(z)$ is inferred from lepton-hadron and lepton-lepton processes, much of this first paper can be viewed as an attempt to predict properties of hadron-hadron collisions from information gained studying lepton-initiated reactions. A subsequent paper will investigate experimental quantities that depend more strongly on the precise form of $d\hat{\sigma}/d\hat{t}$ (e.g., two-particle correlation data in large- p_\perp hadron collisions). Then it will be necessary to include the effects of the transverse momentum spread of the quarks within the hadrons and of the hadrons that fragment from quarks. These effects have little influence on the results of the present paper and we have omitted them in our calculations reported here.

We are fully aware that all partons are not quarks, that half the momentum of the proton is something else (gluons?). And there is no good reason to exclude the possibility that some of the high- p_\perp particles could result from gluon interactions. We are also aware that there is no good reason for the quark-quark cross section to vary as \hat{s}^{-4} . But we must start somewhere and we have chosen to start here. Let us see what experiments might exclude our specific choice, and indicate the presence of gluons, or some different model entirely.

Before we begin, however, we must say ahead of time in what region we expect our theory to hold. We must be careful, because we do not wish to be embarrassed later by appearing to think up an excuse as to why something does not fit. We expect to allow, generally, any data outside the low- p_\perp main collision (for example, outside the low- p_\perp "pionization" region) with enough momentum that our ubiquitous approximations of relativistic quarks and scaling hold. We take this to mean simply the condition $p_\perp \gtrsim 2$ GeV/c, although we can guess that down to 1.5 GeV/c it may still work fairly well. There is one situation where this may be insufficient. If we are calculating something of particularly low probability that is easy to find in the main low- p_\perp part of the collision, we may have to go a little farther out in p_\perp before the "back-

ground" from the main collision falls sufficiently. An example of this is the production in a proton collision of protons of high p_\perp where the large number of protons from the "leading particle effects" in the main collision may spill over into p_\perp beyond 2 GeV/c.

Because of incomplete knowledge of our functions, some things can be predicted with more certainty than others. Those experimental results that are not well predicted can be "used up" to determine these functions in greater detail to permit better prediction of further experiments. Our papers will be a bit long because we wish to discuss this interplay clearly. It is necessary if we are to judge the seriousness of a disagreement with experiment.

We concern ourselves in this paper with large- p_\perp meson production and hope to address the question of proton (or baryon) production at a later date. We begin in Sec. II by determining the distribution of quarks within hadrons. Section III deals with the quark decay functions. Our examination of large- p_\perp hadron-hadron collisions begins in Sec. IV with an investigation of the quark-quark scattering cross section $d\hat{\sigma}/d\hat{t}$. In Sec. V we present the predictions of our model for single-meson production at high p_\perp . Section VI is reserved for a summary and conclusions.

II. THE DISTRIBUTIONS OF QUARKS IN THE INITIAL HADRONS

A. Quark distributions in a proton and neutron

We define $G_{h \rightarrow q}(x)$ as the number of quarks of type q with fraction of momentum between x and $x+dx$ within a hadron of type h of high momentum. In particular, there are six functions which are necessary to describe the quark distributions in a proton:

$$\begin{aligned} u(x) &\equiv G_{p \rightarrow u}(x), \\ d(x) &\equiv G_{p \rightarrow d}(x), \\ s(x) &\equiv G_{p \rightarrow s}(x), \\ \bar{u}(x) &\equiv G_{p \rightarrow \bar{u}}(x), \\ \bar{d}(x) &\equiv G_{p \rightarrow \bar{d}}(x), \\ \bar{s}(x) &\equiv G_{p \rightarrow \bar{s}}(x), \end{aligned} \quad (2.1)$$

where u , d , and s refer to up, down, and strange quarks, respectively, and \bar{u} , \bar{d} , and \bar{s} refer to their antiquarks. These quark distributions satisfy the following sum rules:

$$\int_0^1 [u(x) - \bar{u}(x)] dx = 2, \quad (2.2a)$$

$$\int_0^1 [d(x) - \bar{d}(x)] dx = 1, \quad (2.2b)$$

$$\int_0^1 [s(x) - \bar{s}(x)] dx = 0. \quad (2.2c)$$

That is, the net number of each kind of quark is just the number one arrives at in the simple non-relativistic quark model.² The distribution in a neutron are gotten from isospin symmetry, which implies that $G_{n \rightarrow u}(x) = G_{p \rightarrow d}(x) = d(x)$, $G_{n \rightarrow d}(x) = u(x)$, $G_{n \rightarrow s}(x) = s(x)$, etc. Complete knowledge of the deep-inelastic structure functions for electron and neutrino scattering off protons and neutrons is sufficient to obtain $u(x)$, $d(x)$, $\bar{u}(x)$, $\bar{d}(x)$, and $s(x)$ + $\bar{s}(x)$.³ For instance, with the standard notation,⁴

$$\begin{aligned} \nu W_2^{ep}(x) &= \frac{4}{9}x[u(x) + \bar{u}(x)] + \frac{1}{9}x[d(x) + \bar{d}(x)] \\ &\quad + \frac{1}{9}x[s(x) + \bar{s}(x)], \end{aligned} \quad (2.3a)$$

$$\begin{aligned} \nu W_2^{en}(x) &= \frac{4}{9}x[d(x) + \bar{d}(x)] + \frac{1}{9}x[u(x) + \bar{u}(x)] \\ &\quad + \frac{1}{9}x[s(x) + \bar{s}(x)], \end{aligned} \quad (2.3b)$$

$$\nu W_2^{vp}(x) = 2x[d(x) + \bar{u}(x)], \quad (2.3c)$$

$$\nu W_2^{\bar{v}p}(x) = 2x[u(x) + \bar{d}(x)], \quad (2.3d)$$

$$\nu W_3^{vp}(x) = 2x[\bar{u}(x) - d(x)], \quad (2.3e)$$

$$\nu W_3^{\bar{v}p}(x) = 2x[\bar{d}(x) - u(x)], \quad (2.3f)$$

where we have neglected $\sin^2\theta_C$. We discuss separately the behavior of $G_{p \rightarrow q}(x)$ in the small, medium, and large x region.

1. Medium x range ($0.2 < x < 0.8$)

As is evidenced by ν scattering data \bar{u} , \bar{d} are very small for x beyond about 0.2⁵; we guess the same is true of \bar{s} and s . For $x \gtrsim 0.2$ Eqs. (2.3a) and (2.3b) become

$$\nu W_2^{ep}(x) \approx \frac{4}{9}xu(x) + \frac{1}{9}xd(x), \quad (2.4a)$$

$$\nu W_2^{en}(x) \approx \frac{4}{9}xd(x) + \frac{1}{9}xu(x). \quad (2.4b)$$

The values of $u(x)$ and $d(x)$ resulting from the fits to $\nu W_2^{ep}(x)$ and $\nu W_2^{en}(x)/\nu W_2^{ep}(x)$ shown in Figs. 3(b) and 2 are presented in Fig. 4.

2. Large- x region ($x > 0.8$)

For x near 1 we shall use the Drell-Yan theoretical estimate⁶ that νW_2 goes as $(1-x)^3$, even though experimental indications are that $(1-x)^4$ may be better.⁷ The ratio $\nu W_2^{en}/\nu W_2^{ep}$ is not well known in this region, but as can be seen in Fig. 2 it is falling below 0.4 by $x = 0.8$. There is a theoretical reason (Ref. 2) that suggests it falls to $\frac{1}{4}$ as $x \rightarrow 1$, that is, that $d(x)/u(x) \rightarrow 0$. We assume this and represent these ideas by choosing

$$xu(x) \rightarrow (1-x)^3, \quad (2.5a)$$

$$xd(x) \rightarrow (1-x)^4 \quad (2.5b)$$

as $x \rightarrow 1$.

There is no reliable neutrino information separating \bar{u} from \bar{d} , but the ep data tell us that the integral

$$\int_0^1 [\nu W_2^{ep}(x) - \nu W_2^{en}(x)] \frac{dx}{x} = \int_0^1 \frac{1}{3}(u + \bar{u} - d - \bar{d}) dx \\ = \frac{1}{3} + \frac{2}{3} \int_0^1 (\bar{u} - \bar{d}) dx \quad (2.6)$$

using the sum rules (2.2). Experimentally this integral is hard to determine for it depends on small differences near $x=0$. It seems, however, to be distinctly less than $\frac{1}{3}$ (from the data of Figs. 2 and 3(b) one gets about 0.27), indicating $\bar{u} < \bar{d}$ (although, of course, they must be equal as $x \rightarrow 0$). A likely physical reason for this is the presence of more of what are called "valence" u quarks than

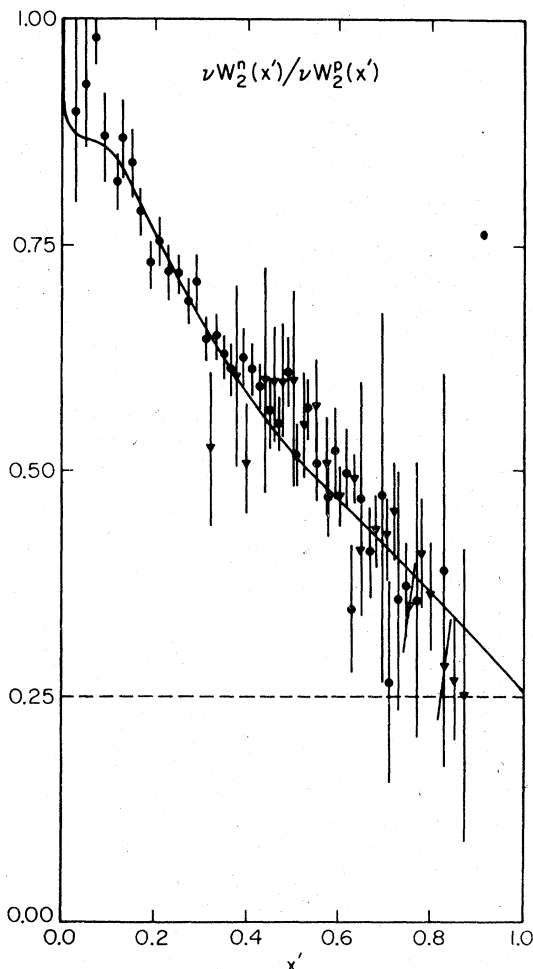


FIG. 2. Fit to $\nu W_2^{en}(x') / \nu W_2^{ep}(x')$ from the quark distributions displayed in Fig. 4, and where we have assumed that as $x \rightarrow 1$ $xu(x) \sim (1-x)^3$ and $xd(x) \sim (1-x)^4$. The data are from A. Bodek *et al.* [Phys. Rev. Lett. 30, 1087 (1973); A. Bodek, M.I.T. thesis, 1973 (unpublished)] (solid circles) and W. B. Atwood [Ph.D. thesis, SLAC Report No. 185, 1975 (unpublished)] (solid triangles).

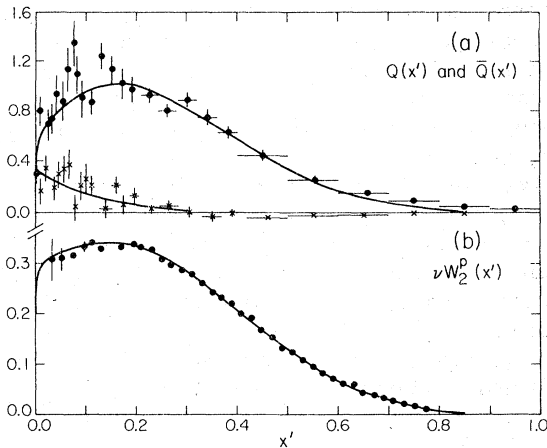


FIG. 3. Comparison of the quark distribution functions (shown in Fig. 4) with data that were used to help determine them. (a) Momentum carried by quarks $Q(x) = xu(x) + xd(x)$, and antiquarks $\bar{Q}(x) = x\bar{u}(x) + x\bar{d}(x)$. The data are from the Gargamelle neutrino collaboration (Ref. 9). (b) Fit to $\nu W_2^{ep}(x')$. The data are from Bodek *et al.* (see caption of Fig. 2).

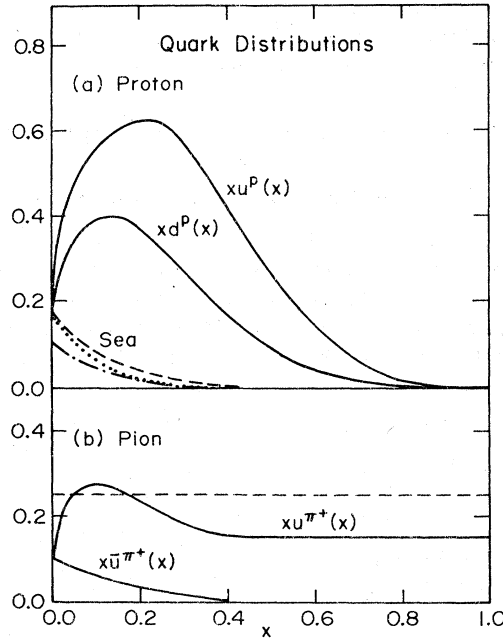


FIG. 4. (a) Quark distribution within the proton. We have assumed that as $x \rightarrow 1$ $xu(x) \sim (1-x)^3$ and $xd(x) \sim (1-x)^4$. In addition, we take an unsymmetrical sea with $xd(x)$ (dashed curve) greater than $x\bar{u}(x)$ (dotted curve) and $xs(x) = x\bar{s}(x) = 0.1 (1-x)^8$ (dash-dot curve). (b) Quark distributions within a pion. As $x \rightarrow 1$ we expect that $xu(\pi^+)(x) \rightarrow$ constant. The dashed curve represents a first guess of $xu(\pi^+)(x) = 0.25$ and $x\bar{u}(\pi^+)(x) = 0$. This is refined by knowledge of large- p_\perp hadron data (Fig. 16) yielding the solid curves.

d quarks, so the pairs $u\bar{u}$ expected to occur in the small x region (the "sea") are suppressed more than $d\bar{d}$ pairs by the exclusion principle. We have no knowledge of the functional form for \bar{u}, \bar{d} except that they fall off very rapidly with x and we have arbitrarily chosen the forms

$$x\bar{u} = c(1-x)^{10}, \quad (2.7a)$$

$$x\bar{d} = c(1-x)^7. \quad (2.7b)$$

This gives 0.28 for the integral above (with $c = 0.17$).

In fact, an even more rapid falloff of these functions, such as e^{-20x} , is also possible. Neutrino experiments which in principle can give us these functions are either at too low energy for the theory to be reliable (1 to 11 GeV at CERN, Ref. 9 and Fig. 3) or of insufficient precision at low x (Fermilab, Ref. 10).

Predictions of the rate that $\mu^+\mu^-$ pairs may be produced in proton-proton collisions are very sensitive to the antiquark content of the proton and these we cannot make reliably. Also, the K^+/K^- ratio produced in hadron collisions at small x_1 is sensitive to the number of antiquarks in the proton.

We have no knowledge of s, \bar{s} and simply choose for our calculations

$$s(x) = \bar{s}(x) = 0.1(1-x)^8. \quad (2.8)$$

3. Small- x region ($x < 0.2$)

For our project this region of x is very rarely of any effect. Nevertheless, for the sake of completeness we have made some specific choices here about which we have, however, little confidence.

One theoretical suggestion¹¹ is that the functions $G(x)$ differ from their $1/x$ behavior by terms of order $1/\sqrt{x}$. This argument comes from imposing "Regge scaling." We know that the $\gamma-p$ photon cross section (which is proportional to νW_2 at $q^2 = 0$) varies as $\alpha + \beta/\sqrt{\nu}$, where α, β are constants. For the neutron α is the same but β is about $\frac{2}{3}$ of that for the proton. In Regge language the first term comes from Pomeron exchange, the second from ρ trajectory. If this is true for virtual γ 's as well, α, β depend on the q^2 of the virtual photon. If this is still true in the scaling region $-q^2/2M\nu = x$ we must have $\nu W_2^{ep} = A + B\sqrt{x}$ and $\nu W_2^{en} + A + B'\sqrt{x}$. Doubt can be expressed as to the legitimacy of interchanging the order of limits ($\nu \rightarrow \infty$ for constant q^2 and $\nu \rightarrow \infty$, $q^2 \rightarrow \infty$ at constant ratio). For example, if β were to vary with q^2 as $1/\sqrt{-q^2}$ (instead of $\sqrt{-q^2}$) the latter term would be of order $(1/q^2)(1/\sqrt{x})$, falling away in the scaling region. Nevertheless, we have chosen to follow the anal-

ysis of Farrar³ and impose Regge behavior for deep-inelastic scattering at $x \rightarrow 0$.

Exchange degeneracy (ϕ and f' decouple from nonstrange baryons) implies that only the "valence" quark distributions have a "Regge" term (\sqrt{x}) at small x . That is, $xu(x) \sim a + b\sqrt{x}$, $xd(x) \sim a + b'\sqrt{x}$, but $x\bar{u}(x) = x\bar{d}(x) \sim a$. The convergence of (2.2a)–(2.2c) requires that $xu = x\bar{u}$, $xd = x\bar{d}$, and $xs = x\bar{s}$ at $x = 0$. The assumed equality $xu = xd$ at $x = 0$ is based on the SU(2)-singlet value of the Pomeron. We do not assume that SU(3) holds exactly and take $xs(x) < xu(x) = 0$ [compare (2.7) and (2.8)]. Our resulting quark distributions are displayed in Fig. 4, where $a = 0.17$, $b = 1.69$, and $b' = 0.78$.¹² The odd shape of these functions below $x = 0.05$ reflects the strains needed to satisfy the sum rules with the Regge parametrization. The dipping of νW_2 as $x \rightarrow 0$ may be wrong, but it does not affect our results.¹³ These choices give, for integrals not sensitive to small x ,

$$\int_0^1 xu(x) dx = 0.285, \quad (2.9a)$$

$$\int_0^1 xd(x) dx = 0.145, \quad (2.9b)$$

$$\int_0^1 x\bar{u}(x) dx = 0.015, \quad (2.9c)$$

$$\int_0^1 x\bar{d}(x) dx = 0.021, \quad (2.9d)$$

$$\int_0^1 xs(x) dx = \int_0^1 x\bar{s}(x) dx = 0.011. \quad (2.9e)$$

The total momentum carried by the quarks and antiquarks within the proton is about 49% and the ratio of momentum carried by antiquarks compared to quarks is 11%.

B. Quark distributions in the pion

During the course of this paper we will need to know the quark distributions in a pion $G_{\pi-q}(x)$. Since there is no experimental information on $\nu W_2^{\pi\pi}(x)$ we are forced to estimate $G_{\pi-q}(x)$ entirely on theoretical prejudices. Let us continue to assume the connection between the behavior of $\nu W_2^{\pi\pi}(x)$ near $x = 1$ and the form factors $F_{h-h}(Q^2)$ as interpreted in the parton model.⁶ For the case of the proton the elastic form factor $F_{p-p}(Q^2)$ and the transition form factors $F_{p-N}(Q^2)$ (N has isospin $\frac{1}{2}$) all behave like Q^{-4} and each contributes to the scaling limit like $(1-x)^3$. For the pion, on the other hand, the situation is altered by the fact that the pion has spin 0, while the quark has spin $\frac{1}{2}$ (for the proton both have spin $\frac{1}{2}$). This mismatch of spins results in a pion elastic form factor $F_{\pi-\pi}(Q^2)$ which falls off faster by one power of Q

than does the transition form factor $F_{\pi \rightarrow h}(Q^2)$ when h does not have spin zero (i.e., ρ , ω , A_2 , etc.). This is because only longitudinally polarized virtual photons (zero angular momentum about their direction of momentum, say) contribute to the form factor, while transversely polarized ones (angular momentum ± 1) contribute to the $\pi \rightarrow \rho$, etc. Relativistically, longitudinal photons couple to a fast quark at a relative amplitude of $1/Q$. To conserve angular momentum about z they must either change the quark helicity (only if the quark has a mass, amplitude m/Q), or use one unit of orbital angular momentum of the quark about z (amplitude Q_1/Q where Q_1 is the component of quark momentum, assumed finite, in the xy plane). Thus

$$F_{\pi \rightarrow \pi}(Q^2) \propto F_{\pi \rightarrow h}(Q^2)/Q, \quad (2.10)$$

which means [for we assume that the pion form factor $F_{\pi \rightarrow \pi}(Q^2)$ falls at $1/Q^2$] that the leading power behavior γ of $G_{\pi \rightarrow q}(x) \sim (1-x)^\gamma$ near $x=1$ is not $\gamma=1$, as would be the case if only the elastic form factor contributed to $\nu W_2^{e\pi}(x)$, but is instead $\gamma=0$ resulting from the contributions of the transition form factors.^{14,15} We thus assume that

$$xu^{\pi^+}(x) \xrightarrow[x \rightarrow 1]{} C_\pi \text{ (a constant)}, \quad (2.11)$$

where we have written $u^{\pi^+}(x)$ for $G_u^{\pi^+}(x)$. [It is equal to $G_d^{\pi^+}(x)$ by charge conjugation and isospin symmetry.] In fact, as a first naive guess we will take $xu^{\pi^+}(x)$ to be constant over the entire x range. In this case the total fraction of momentum carried by the $u+\bar{d}$ quarks within the π^+ is $2C_\pi$. For pions this number is of course not known, but guessing that it is the same as the total fraction of momentum carried by all quarks within the proton (about 50%) yields $C_\pi=0.25$. As discussed in Sec. V B these crude assumptions result in a prediction for the large- ρ_\perp beam ratio $\sigma(pp \rightarrow \pi^0 X)/\sigma(\pi p \rightarrow \pi^0 X)$ that has the qualitative features of the data but is off somewhat in the normalization. The value of 0.25 is too large. Knowing this we can construct more sophisticated pion structure functions.

The Regge formalism in the small x region suggests (omitting small effects of possible differences of s quark content in π^+ and p)

$$\begin{aligned} xu(x)/xu^{\pi^+}(x) &\sim \sigma_{\text{tot}}(\gamma_\nu p)/\sigma_{\text{tot}}(\gamma_\nu \pi^+) \\ &\approx \sigma_{\text{tot}}(pp)/\sigma_{\text{tot}}(\pi^+ p) \approx 1.7, \end{aligned} \quad (2.12)$$

where γ_ν refers to a virtual photon. We thus take $xu^{\pi^+}(x)=0.1$ at $x=0$. In addition, we include the nonvalence distributions

$$x\bar{u}^{\pi^+}(x)=0.1(1-x)^5 \quad (2.13)$$

(isospin and charge conjugation make $d^{\pi^+}=\bar{u}^{\pi^+}$ and $s^{\pi^+}=\bar{s}^{\pi^+}$) and adjust the small- x behavior of $xu^{\pi^+}(x)$

to satisfy the sum rule

$$\int_0^1 [u^{\pi^+}(x) - \bar{u}^{\pi^+}(x)] dx = 1. \quad (2.14)$$

The value of C_π in (2.11) is adjusted to 0.15 to give the proper normalization for the beam ratio, $\sigma(pp \rightarrow \pi^0 X)/\sigma(\pi p \rightarrow \pi^0 X)$ (see Sec. V B). The final quark distributions within a pion are shown in Fig. 4(b) and yield

$$\int_0^1 [xu^{\pi^+}(x) + x\bar{d}^{\pi^+}(x)] dx = 0.354, \quad (2.15a)$$

$$\int_0^1 x\bar{d}^{\pi^+}(x) dx = 0.017, \quad (2.15b)$$

and for simplicity we take $d^{\pi^+}(x)=s^{\pi^+}(x)=\bar{s}^{\pi^+}(x)$. The total fraction of momentum carried by the quarks within the pion is about 42% (7% corresponds to "wrong quarks" d, \bar{u}, s, \bar{s}) compared with about 49% for the proton.

III. QUARK DECAY DISTRIBUTIONS $D_q^h(z)$

A. Definition

We now turn to discuss another element of our model, the way quarks make hadrons. We assume that a quark of a particular flavor q moving away from other quarks with a large momentum P fragments into a cascade of hadrons, all of which have small momentum transverse to P . The number of hadrons of type h with momentum fraction z (i.e., with component in the direction of P of magnitude zP) per dz , which we call $D_q^h(z)$, is independent of how the quark q was produced or of its color. The total momentum of all the hadrons must be that of the quark (neglecting the momentum of γ rays not identified as coming from π^0 , such as $\eta \rightarrow 2\gamma$ or $\omega \rightarrow \pi^0\gamma$)

$$\sum_h \int_0^1 z D_q^h(z) dz = 1. \quad (3.1)$$

The integral of $D_q^h(z)$ itself counts each type of hadron repeatedly so that

$$\int_{z_{\min}}^1 D_q^h(z) dz \quad (3.2)$$

is the mean multiplicity of particles of type h emerging from the parent quark q with $z > z_{\min}$. Since near $z=0$ these decay functions rise as $1/z$, the multiplicity above a given fixed momentum P_0 ($z_{\min}=P_0/P$) rises logarithmically with the quark momentum P .

Ideally these decay functions, not depending on the origin of the quark, could be determined by lepton collisions—particularly by studying the hadrons in the recoil direction in neutrino (and

antineutrino) reactions such as $\nu p \rightarrow \mu^- + h + X$, where we know (for large $x = -q^2/2M\nu$ at least) what kind of quark (here u) comes out (see Fig. 1). Unfortunately present experiments, which we will discuss in a moment, are incomplete so we shall have to supplement them by theoretical guesses.

The theoretical picture which we use to guide our thinking is this: As the quark q (presumably colored) leaves the others, the forces responsible for confinement build up an ever larger field until pairs of quarks q, \bar{q} are produced which breaks down the field. The many quarks and antiquarks produced now gather into color singlets, $q\bar{q}$ and qqq forming hadrons. These ideas are discussed by Bjorken¹⁶ and analyzed in a one-dimensional model by Casher, Kogut, and Susskind.¹⁷ Of course these hadrons such as N^* , ρ may undergo further rapid disintegration until they become the more stable hadrons which we observe (i.e., π, K, N).

The field (color field?), since it is independent of the flavor of q , makes new pairs in a manner independent of q . The original quark finds itself in one of the hadrons near the higher end of the momentum distribution, in particular if z is near 1 so that one hadron carries most of the available momentum that hadron contains the original quark. The lower z hadrons are distributed in a way that gradually becomes independent of q as z falls, and are ultimately uniform in rapidity ($\ln z$). The new quark pairs are equally likely to be $\bar{u}u$ and $\bar{d}d$, from isospin symmetry—but SU(3) is not assumed. Thus, if we suppose strange quarks have a higher intrinsic mass than nonstrange quarks, the rate of $\bar{s}s$ pair production by the field would be lower than $\bar{u}u$ or $\bar{d}d$ production. We disregard, for our purposes, the rare production of charmed quarks or other flavors.

We add one further assumption originally suggested to us by Cisneros² and studied extensively in the literature.¹⁸ For $z \rightarrow 1$ in $D_q^h(z)$ we are asking for the probability that a quark q looks nearly like a pure hadron h and some stuff at small momentum (of total only $1-z$). In $G_{h+q}(x)$ for $x \rightarrow 1$ we ask that a hadron of type h look almost like a pure quark and stuff at small momentum (total $1-x$). We assume the same functional behavior as z (or x) $\rightarrow 1$ [i.e., if $G_{h+q} = c(1-x)^\gamma$ as $x \rightarrow 1$ then $D_q^h(z) = c'(1-z)^\gamma$ with the same γ as $z \rightarrow 1$]. Theoretical arguments have been given to suggest that perhaps even the coefficients c, c' may be equal.^{18,19}

B. Pions resulting from quark decay

Isospin and charge-conjugation invariance reduces the number of independent D_q^π functions to

three:

$$D_u^{\pi^+}(z) = D_d^{\pi^+}(z) = D_{\bar{u}}^{\pi^+}(z) = D_{\bar{d}}^{\pi^+}(z), \quad (3.3a)$$

$$D_d^{\pi^+}(z) = D_u^{\pi^+}(z) = D_{\bar{d}}^{\pi^+}(z) = D_{\bar{u}}^{\pi^+}(z), \quad (3.3b)$$

$$D_s^{\pi^+}(z) = D_s^{\pi^-}(z) = D_{\bar{s}}^{\pi^+}(z) = D_{\bar{s}}^{\pi^-}(z), \quad (3.3c)$$

In every case $D_q^{\pi^0} = (D_q^{\pi^+} + D_q^{\pi^-})/2$.

We shall try to limit the number of unknowns to two by taking $D_s^{\pi^+}(z) = D_d^{\pi^+}(z)$. This assumption is based on the idea that $D_s^{\pi^+}(z)$ and $D_d^{\pi^+}(z)$ are both unfavored with respect to $D_u^{\pi^+}(z)$ since π^+ contains an up-quark and can thus be formed directly from u by combining with a \bar{d} , whereas an s or d quark can make a π^+ only through an intermediate state (such as $d \rightarrow \rho^0 \rightarrow \pi^+$) or by producing it further down the cascade. That is, to make π^+ ($= u\bar{d}$) from either s or d quarks requires the creation of two quarks of new flavors u and \bar{d} . This is not meant to be exact; for example, η 's disintegrating into π^+ are unequally made by s and d quarks, or again d can make ρ_0 (with a new \bar{d}) and $\rho \rightarrow \pi^+\pi^-$, whereas the corresponding process $s \rightarrow \bar{K}^{0*} \rightarrow K^+ + \pi^+$ may not have equal probability. But in view of the limited data available it is a reasonable first guess to make, in order to limit the possibilities.

We take as unknowns the two functions

$$D(z) \equiv D_u^{\pi^+}(z) + D_u^{\pi^-}(z) = 2D_u^{\pi^0}(z) \quad (3.4)$$

and the π^-/π^+ ratio from an up quark,

$$\omega(z) \equiv D_u^{\pi^-}(z)/D_u^{\pi^+}(z). \quad (3.5)$$

C. Kaons resulting from quark decay

For the production of K mesons there are six independent functions $D_q^{K^+}(z)$; the others are obtained by isospin and charge conjugation; for example, $D_u^{K^+} = D_{\bar{u}}^{K^+} = D_d^{K^+} = D_{\bar{d}}^{K^+} = D_s^{K^+} = D_{\bar{s}}^{K^+}$. We have little information and will reduce them by approximate arguments. First, we may expect $D_s^{K^+} = D_d^{K^+}$ because in each case for the K^+ we must make two new quarks \bar{s}, u unrelated to the s or d . Again, we expect $D_{\bar{u}}^{K^+} = D_{\bar{d}}^{K^+}$ for the same reason. However, we think $D_d^{K^+} > D_{\bar{d}}^{K^+}$ because starting with a d quark the new pairs $\bar{s}s$ may always have the \bar{s} quark of higher momentum than the s (for that is the direction of the field making the new pairs). Starting with the \bar{d} the s is higher so K^+ is easier to make at high momentum from d than \bar{d} . The effect is partly compensated by a similar effect for the $\bar{u}u$ pair [and is zero in SU(3)]. We have no experimental clue of the strength of the effect and have chosen, for the sake of simplicity, to disregard it and reduce our functions to three by setting

$$D_s^{K^+}(z) = D_d^{K^+}(z) = D_{\bar{u}}^{K^+}(z) = D_{\bar{d}}^{K^+}(z). \quad (3.6)$$

In addition, for simplicity we take

$$D_u^{K^-}(z)/D_u^{K^+}(z) = \omega(z), \quad (3.7)$$

where $\omega(z)$ is the same as used in (3.5). We also assume that

$$D_{\bar{s}}^{K^+}(z)/D_{\bar{d}}^{\pi^+}(z) \xrightarrow[z \rightarrow 1]{} 1, \quad (3.8)$$

supposing that as $z \rightarrow 1$ it is just as easy for an \bar{s} quark to pick up a u quark and become a K^+ as it is for a \bar{d} quark to pick up a u quark and become a π^+ .

In the small- z "plateau" region the K^+ meson no longer "remembers" that it originated from a u or \bar{s} quark so that

$$D_u^{K^+}(z)/D_{\bar{s}}^{K^+}(z) \xrightarrow[z \rightarrow 0]{} 1. \quad (3.9)$$

However, we do not assume that $D_u^{K^+} = D_{\bar{s}}^{K^+}$ in general because it might be harder to make new $\bar{s}s$ pairs than $\bar{u}u$ pairs because of the mass of the s quark, making $D_u^{K^+}(z) < D_{\bar{s}}^{K^+}(z)$ for large z . We have no way to guess at the amount of this SU(3) breaking, but we have determined

$$D_u^{K^+}(z)/D_{\bar{s}}^{K^+}(z) \xrightarrow[z \rightarrow 1]{} 0.5 \quad (3.10)$$

to fit the experimental result that $\sigma(pp \rightarrow K^+X)/\sigma(pp \rightarrow \pi^+X)$ is about 0.5 at large x_1 (see Sec. V C).

We choose our two independent kaon decay functions to be

$$K_u(z) \equiv D_u^{K^+}(z) + D_u^{K^-}(z)$$

and

$$K_s(z) \equiv D_s^{K^+}(z) + D_s^{K^-}(z). \quad (3.12)$$

D. Baryons resulting from quark decay

Finally we have little information on baryon production and will leave the functions D_q^p , $D_{\bar{q}}^{\bar{p}}$, etc. to a later study. We do know they are relatively small, however, and that in many experiments protons are not distinguished from K^+ or even π^+ , so for a while we shall even forget their contribution to the normalization of total momentum, etc., disregarding them altogether.

E. Sum rule constraints on $D_q^h(z)$

With the above crude assumptions we can relate all the meson decay functions $D_q^h(z)$ to the four functions $D(z)$, $K_u(z)$, $K_s(z)$, and $\omega(z)$ as shown in Table I. Further constraints on these functions come from the momentum sum rule (3.1) which, using Table I, reduces to the two conditions (for $q=u$ and $q=s$)

$$\int_0^1 z \left[\frac{3}{2} D + (1 + 3\omega) K_u / (1 + \omega) \right] dz = 1, \quad (3.13a)$$

$$\int_0^1 z [3\omega D / (1 + \omega) + 2K_s] dz = 1. \quad (3.13b)$$

In addition, charge symmetry implies the isospin

sum rule

$$\begin{aligned} \int_0^1 & \{ [D_q^{\pi^+}(z) - D_q^{\pi^-}(z)] + \frac{1}{2} [D_q^{K^+}(z) - D_q^{K^-}(z)] \\ & + \frac{1}{2} [D_{\bar{q}}^{\bar{K}^0}(z) - D_{\bar{q}}^{K^0}(z)] \} dz = I_q, \end{aligned} \quad (3.14)$$

where I_q is the third component of isospin for quark q . Our decay function were constrained to satisfy (3.13a), (3.13b), and (3.14).

The total charge of all hadrons need not be equal to the charge on the quark, as pointed out by Farrar and Rosner.²⁰ Owing to SU(3) breaking, there is a possible "polarization" of the plateau region (K^+ always at higher momentum than K^- , for example). This should reduce the charge for u quarks a bit below $\frac{2}{3}$, and reduce it for d and s quarks by the same amount below $-\frac{1}{3}$, disregarding baryons. The decay distributions resulting from our analysis, in fact, yield

$$\int_0^1 (D_u^{\pi^+} - D_u^{\pi^-} + D_u^{K^+} - D_u^{K^-}) dz = 0.59, \quad (3.15a)$$

$$\int_0^1 (D_d^{\pi^+} - D_d^{\pi^-} + D_d^{K^+} - D_d^{K^-}) dz = -0.40, \quad (3.15b)$$

$$\int_0^1 (D_s^{\pi^+} - D_s^{\pi^-} + D_s^{K^+} - D_s^{K^-}) dz = -0.39. \quad (3.15c)$$

F. Single-hadron production in neutrino and antineutrino reactions—determination of $\omega(z) \equiv D_u^{\pi^+}(z)/D_u^{\pi^+}(z)$

The quark-parton model²¹ predicts that the cross section for $LN \rightarrow l' + h + X$ is completely specified by the probabilities of finding quarks of type q within the nucleon $G_{N-q}(x)$ and the decay distributions of the quarks of type q' (q is converted to q' by the l, l' transition) into the hadron h , $D_q^h(z)$. Neglecting $\sin^2 \theta_C$ one arrives at

$$d\sigma/dxdz(\nu p \rightarrow \mu^- + h + X) = 2x [d(x)D_u^h(z) + \frac{1}{3}\bar{u}(x)D_{\bar{d}}^h(z)], \quad (3.16a)$$

$$d\sigma/dxdz(\bar{\nu}p \rightarrow \mu^+ + h + X) = 2x [\frac{1}{3}u(x)D_d^h(z) + \bar{d}(x)D_{\bar{u}}^h(z)], \quad (3.16b)$$

$$d\sigma/dxdz(\nu n \rightarrow \mu^- + h + X) = 2x [u(x)D_u^h(z) + \frac{1}{3}\bar{d}(x)D_{\bar{d}}^h(z)], \quad (3.16c)$$

$$d\sigma/dxdz(\bar{\nu}n \rightarrow \mu^+ + h + X) = 2x [\frac{1}{3}d(x)D_d^h(z) + \bar{u}(x)D_{\bar{u}}^h(z)], \quad (3.16d)$$

where cross sections are in units of $G^2 ME/\pi$ and $x = -q^2/(2q \cdot p)$ (q and p represent the four-momentum of the lepton current and initial nucleon, respectively), and $z = E_h/\nu$ is the fraction of energy transfer carried by the observed hadron. Specializing to the case of π^+ production (3.16a)–(3.16d) become

TABLE I. Quark decay functions $D_q^h(z)$, where we define $D(z) = D_u^{\pi^+}(z) + D_u^{\pi^-}(z)$, $K_u(z) = D_u^{K^+}(z) + D_u^{K^-}(z)$, $K_s(z) = D_s^{K^+}(z) + D_s^{K^-}(z)$, and $\omega(z) = D_u^{\pi^+}(z)/D_u^{\pi^+}(z)$.

$q \setminus h$	π^+	π^0	π^-	K^+	K^0	K^-	\bar{K}^0
u	$D/(1+\omega)$	$\frac{1}{2}D$	$\omega D/(1+\omega)$	$K_u/(1+\omega)$	$\omega K_u/(1+\omega)$	$\omega K_u/(1+\omega)$	$\omega K_u/(1+\omega)$
d	$\omega D/(1+\omega)$	$\frac{1}{2}D$	$D/(1+\omega)$	$\omega K_u/(1+\omega)$	$K_u/(1+\omega)$	$\omega K_u/(1+\omega)$	$\omega K_u/(1+\omega)$
s	$\omega D/(1+\omega)$	$\omega D/(1+\omega)$	$\omega D/(1+\omega)$	$\omega K_u/(1+\omega)$	$\omega K_u/(1+\omega)$	$K_s - \omega K_u/(1+\omega)$	$K_s - \omega K_u/(1+\omega)$
\bar{u}	$\omega D/(1+\omega)$	$\frac{1}{2}D$	$D/(1+\omega)$	$\omega K_u/(1+\omega)$	$\omega K_u/(1+\omega)$	$K_u/(1+\omega)$	$\omega K_u/(1+\omega)$
\bar{d}	$D/(1+\omega)$	$\frac{1}{2}D$	$\omega D/(1+\omega)$	$\omega K_u/(1+\omega)$	$\omega K_u/(1+\omega)$	$\omega K_u/(1+\omega)$	$K_u/(1+\omega)$
\bar{s}	$\omega D/(1+\omega)$	$\omega D/(1+\omega)$	$\omega D/(1+\omega)$	$K_s - \omega K_u/(1+\omega)$	$K_s - \omega K_u/(1+\omega)$	$\omega K_u/(1+\omega)$	$\omega K_u/(1+\omega)$

$$d\sigma/dxdz(\nu N \rightarrow \mu^- + \pi^+ + X) = D_u^{\pi^+}(z)[Q(x) + \frac{1}{3}\bar{Q}(x)] , \quad (3.17a)$$

$$d\sigma/dxdz(\nu N \rightarrow \mu^- + \pi^- + X^-) = D_u^{\pi^-}(z)[Q(x) + \frac{1}{3}\bar{Q}(x)] , \quad (3.17b)$$

$$d\sigma/dxdz(\bar{\nu} N \rightarrow \mu^+ + \pi^+ + X) = D_u^{\pi^+}(z)[\frac{1}{3}Q(x) + \bar{Q}(x)] , \quad (3.17c)$$

$$d\sigma/dxdz(\bar{\nu} N \rightarrow \mu^+ + \pi^- + X) = D_u^{\pi^+}(z)[\frac{1}{3}Q(x) + \bar{Q}(x)] , \quad (3.17d)$$

where we used the relationships given in (3.3a)–(3.3c) and where the target N is an average over neutron and proton $N = (n+p)/2$, and

$$\begin{aligned} Q(x) &= x(u(x) + d(x)) , \\ \bar{Q}(x) &= x(\bar{u}(x) + \bar{d}(x)) \end{aligned} \quad (3.18)$$

are the momentum distributions of nonstrange quarks and antiquarks in the proton. Thus we expect the π^+/π^- ratio with a neutrino beam and the π^-/π^+ ratio for an antineutrino beam should be equal and independent of x ,

$$\pi^+/\pi^-(\nu) = \pi^-/\pi^-(\bar{\nu}) = 1/\omega(z) , \quad (3.19)$$

$$\frac{\pi^+}{\pi^-}(ep) = \frac{[4u(x) + \bar{d}(x)] + \omega(z)[d(x) + s(x) + \bar{s}(x) + 4\bar{u}(x)]}{[4\bar{u}(x) + d(x)] + \omega(z)[4u(x) + s(x) + \bar{s}(x) + \bar{d}(x)]} \quad (3.20b)$$

$$\frac{\pi^+}{\pi^-}(en) = \frac{[4d(x) + \bar{u}(x)] + \omega(z)[u(x) + s(x) + \bar{s}(x) + 4\bar{d}(x)]}{[4\bar{d}(x) + u(x)] + \omega(z)[4d(x) + s(x) + \bar{s}(x) + \bar{u}(x)]} \quad (3.20c)$$

In contrast to the neutrino case these ratios depend on both z and x . A naive guess that $\omega(z) = 0$ and $u(x) = 2d(x)$ and no sea yields $\pi^+/\pi^-(ep) = 8$ and $\pi^+/\pi^-(en) = 2$. The data^{27–29} show this clearly not to be the case. In fact, using the quark distributions $G_{N \rightarrow q}(x)$ determined in Sec. II A, and the ratio $\omega(z)$ determined from neutrino reactions, Sec. III F, we can predict the π^+/π^- ratios for eN scattering

where $\omega(z) = D_u^{\pi^+}(z)/D_u^{\pi^+}(z)$ is defined in (3.5). The π^+/π^- ratio in neutrino and antineutrino scattering is thus a direct measure of the quantity $\omega(z)$ in a way that does not depend on the behavior of the quark probabilities $Q(x)$ or $\bar{Q}(x)$.^{22–25}

The experimental results²² shown in Fig. 5 are consistent with what we expect; $\omega(z) \rightarrow 1$ as $z \rightarrow 0$ and $\omega(z) \rightarrow 0$ as $z \rightarrow 1$. The solid curve in Fig. 5 is our parametrization of $1/\omega(z)$ and is used throughout the paper.²⁶ Figure 5(b) shows that the π^+/π^- ratio (3.19) is indeed independent of x as required, and the line is the predicted value using our $\omega(z)$ as determined in Fig. 5(a).

G. Single-hadron production in electron reactions—check of quark-patron-model approach

Within the quark-parton model the cross section for π^\pm production in electron-nucleon scattering (see Fig. 1) is derived analogously (3.16a)–(3.16d) except now the charges of the quark must be considered.^{27,28} Defining

$$\pi^+/\pi^-(eN) = \frac{d\sigma/dxdz(eN - e\pi^+X)}{d\sigma/dxdz(eN - e\pi^-X)} , \quad (3.20a)$$

one arrives at

$$(3.20b)$$

(3.20b) and (3.20c) with no free parameters. The predictions are consistent with the data as can be seen by examining the multiplicity functions in Fig. 7.

H. Determination of the magnitudes of $D(z)$, $K_u(z)$, and $K_s(z)$

The multiplicity of hadrons h in $IN \rightarrow l' + h + X$ is defined by

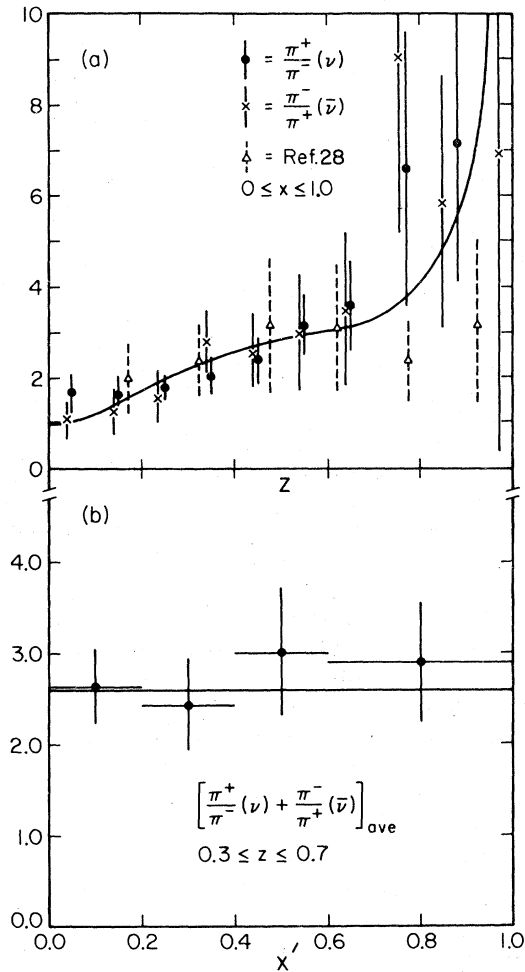


FIG. 5. (a) Fit to the neutrino- (antineutrino-) induced ratio π^+/π^- (π^-/π^+) versus z . The data are from the Gargamelle neutrino collaboration (Ref. 22). The curve is $1/\omega(x) = D_u^{\pi^+}(z)/D_u^{\pi^-}(z)$ and the open triangles are the determination of $1/\omega(z)$ by Sehgal (Ref. 28), who used data on $ep \rightarrow (\pi^+/\pi^-) + X$. (b) It is predicted that the π^+/π^- ratio for neutrinos (and for antineutrinos) does not depend on x' . We plot versus x' the ratio $[\pi^+/\pi^-(\nu) + \pi^-/\pi^+(\bar{\nu})]$ averaged over the z range $0.3 \leq z \leq 0.7$. The data are from the Gargamelle neutrino collaboration (Ref. 22).

$$N_{IN}^h(lN \rightarrow l' + h + X; x, y, z) = \frac{\sigma^h(l + N - l' + h + X; x, y, z)}{\sigma_{\text{tot}}(lN \rightarrow l'; x, y)}, \quad (3.21)$$

where $x = Q^2/2M\nu$, $y = \nu/E$, and $z = E_h/\nu$. For neutrino-proton interactions we have simply (neglecting $\sin^2\theta_C$ for antiquark contributions)

$$N_{\nu p}^{\pi^\pm}(x, z) = D_u^{\pi^\pm}(z) \quad (3.22a)$$

and

$$N_{\nu p}^{\pi^+}(x, z) + N_{\nu p}^{\pi^-}(x, z) = D(z), \quad (3.22b)$$

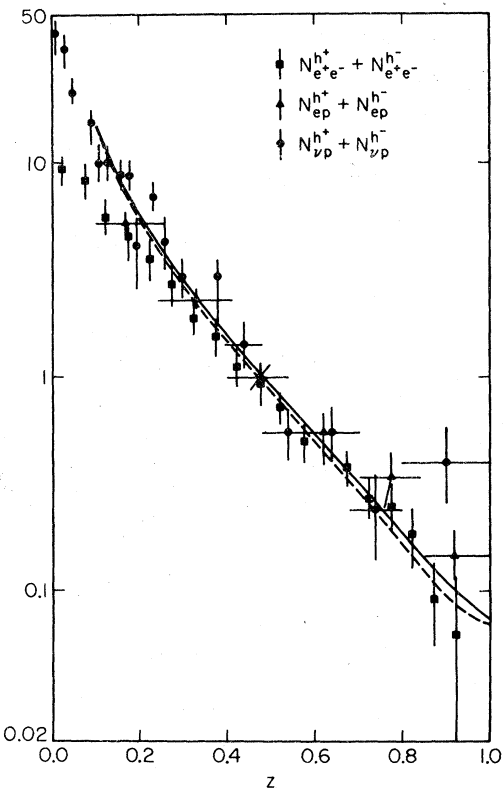


FIG. 6. To determine the magnitudes of the quark decay functions $D(z) = D_u^{\pi^+}(z) + D_u^{\pi^-}(z)$, $K_u(z) = D_u^{K^+}(z) + D_u^{K^-}(z)$, and $K_s(z) = D_s^{K^+}(z) + D_s^{K^-}(z)$, we examine the z dependence of the experimental multiplicity functions $N_{e^+e^-}^{h^+} + N_{e^+e^-}^{h^-}$ for $e^+e^- \rightarrow h^\pm + X$ at $W = 3.0$ GeV [R. F. Schwitters, in *Proceedings of the 1975 International Symposium on Lepton and Photon Interactions at High Energies, Stanford, California*, edited by W. T. Kirk (SLAC, Stanford, 1976), p. 5; Gail Hanson, invited talk presented at the VII International Colloquium on Multiparticle Reactions, Munich, Germany, 1976 (unpublished)], and $N_{ep}^{h^+} + N_{ep}^{h^-}$ for $ep \rightarrow h^\pm + X$ for the range $12 < s < 30$ GeV^2 , $1.0 \leq Q^2 \leq 2.0$ GeV^2 from Ref. 29, and $N_{\nu p}^{h^+} + N_{\nu p}^{h^-}$ for $30 < E < 200$ GeV [J. C. Vander Velde, talk presented at the Fourth International Winter Meeting on Fundamental Physics, Salardu, Spain, 1976 (unpublished); J. P. Berge et al., Fermilab report, 1975 (unpublished); A. A. Seidl, talk presented at the VII International Colloquium on Multiparticle Reactions, Munich, 1976 (unpublished)]. According to the quark-parton model (Fig. 1) these multiplicities should all roughly agree. The solid (dashed) curve is our fit to $N_{\nu p}^{h^+} + N_{\nu p}^{h^-}$ ($N_{e^+e^-}^{h^+} + N_{e^+e^-}^{h^-}$). Our fit to the electroproduction lies between these curves.

where $D(z)$ is defined in (3.4). Similarly for $ep \rightarrow e + h^\pm + X$ we have

$$N_{ep}^{h^\pm}(x, z) = \frac{1}{f_{ep}(x)} \left\{ \left[\frac{4}{9} u(x) + \frac{1}{9} \bar{d}(x) \right] D_u^{h^\pm}(z) + \left[\frac{4}{9} \bar{u}(x) + \frac{1}{9} d(x) \right] D_d^{h^\pm}(z) + \frac{1}{9} [s(x) + \bar{s}(x)] D_s^{h^\pm}(z) \right\},$$

where

$$\begin{aligned} f^{ep}(x) = & \frac{4}{9} [u(x) + \bar{u}(x)] + \frac{1}{9} [d(x) + \bar{d}(x)] \\ & + \frac{1}{9} [s(x) + \bar{s}(x)]. \end{aligned}$$

Therefore

$$\begin{aligned} N_{ep}^{h^+}(x, z) + N_{ep}^{h^-}(x, z) &= D_u^{h^+}(z) + D_u^{h^-}(z) \\ &+ \frac{1}{f^{ep}(x)} \frac{1}{9} [s(x) + \bar{s}(x)] (2D_s^{h^+} - D_u^{h^+} - D_u^{h^-}). \end{aligned}$$

Neglecting the small s, \bar{s} contribution yields

$$N_{ep}^{h^+}(x, z) + N_{ep}^{h^-}(x, z) \approx D(z). \quad (3.23)$$

The cross section for charged-hadron production in e^+e^- collisions is also quite simple in the quark model below the threshold for producing charm or new particles (see Fig. 1). We define multiplicity functions for the process $e^+e^- \rightarrow h^\pm + X$,

$$N_{e^+e^-}^{h^\pm}(z) = \frac{1}{2\sigma_{\text{tot}}} \frac{d\sigma}{dz} (e^+e^- \rightarrow h^\pm + X), \quad (3.24)$$

which are related to the quark decay function by

$$\begin{aligned} N_{e^+e^-}^{h^+}(z) + N_{e^+e^-}^{h^-}(z) &= \frac{2}{3} [D_u^{h^+}(z) + D_u^{h^-}(z)] \\ &+ \frac{1}{6} [D_d^{h^+}(z) + D_d^{h^-}(z)] \\ &+ \frac{1}{6} [D_s^{h^+}(z) + D_s^{h^-}(z)], \quad (3.25) \end{aligned}$$

where $z = 2p_h/E_{\text{c.m.}}$. Assuming that the only charged particles are π^\pm and K^\pm and using Table I

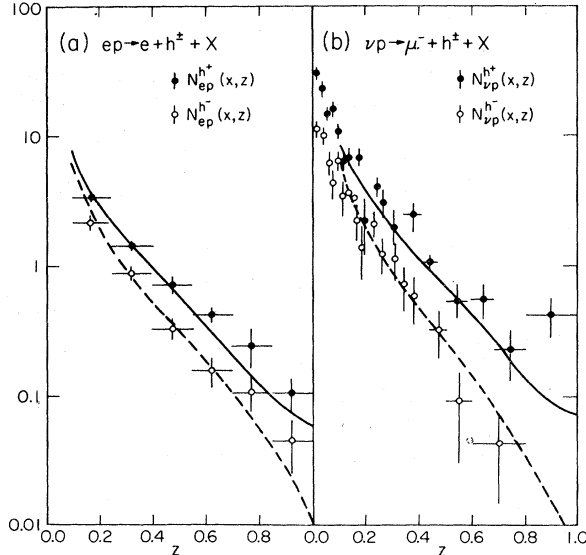


FIG. 7. (a) Predictions of the separate multiplicity functions $N_{ep}^{h^+}$ and $N_{ep}^{h^-}$ for $ep \rightarrow h^\pm + X$ compared with data for the range $12 < s < 30 \text{ GeV}^2$, $1.0 < Q^2 < 2.0 \text{ GeV}^2$ from Ref. 29. (b) Predictions of the separate multiplicity functions $N_{\nu p}^{h^+}$ and $N_{\nu p}^{h^-}$ compared with data for $30 < E < 200 \text{ GeV}$ (from works cited in the caption of Fig. 6).

yields

$$\begin{aligned} N_{e^+e^-}^{h^+}(z) + N_{e^+e^-}^{h^-}(z) &= \frac{5}{6} D(z) + \frac{2}{3} K_u(z) + \frac{1}{6} K_s(z) \\ &+ \frac{1}{3} \omega(z) [D(z) + K_u(z)] / (1 + \omega). \end{aligned} \quad (3.26)$$

Neglecting kaons and the small s, \bar{s} contributions the $\pi^+ + \pi^-$ multiplicity functions for νp [(3.22b)], ep [(3.23)], and e^+e^- [(3.26)] should all agree. A comparison of the data is shown in Fig. 6.³⁰ Unfortunately the ep data are not at as high an energy ($Q^2 \sim 2 \text{ GeV}^2$) as we should like and the e^+e^- data are taken at the low value of $W = 3.0 \text{ GeV}$ to avoid contamination from other possible quark flavors or heavy leptons; nevertheless, the agreement is good. We have used the data in Fig. 6 and Eqs. (3.25) and (3.26) together with the sum rule constraints (3.13a), (3.13b), and (3.14) to estimate the functions $D(z)$, $K_u(z)$, and $K_s(z)$. The value of $D(z)$ at $z = 1$ is not well determined by the data of Fig. 6. We find that setting $D^{h^+}(z = 1) = G_{\pi^+ \rightarrow u}(x = 1)/3 = 0.05$ [see Fig. 4(b), the factor $\frac{1}{3}$ is for color] yields a satisfactory fit to the data, and thus we assume this equality throughout the paper. The $K_u(z)$ and $K_s(z)$ functions are arrived at by using (3.8), (3.9), and (3.10) along with the sum rules (3.13a), (3.13b), and (3.14). All three functions were initially hand-drawn and later these hand-drawn curves were fitted according to the parametrization given in Table VI.⁵⁶ In Fig. 7, for completeness, we compare the separate multiplicities for h^+ and h^- production in νp and ep collisions resulting from our decay func-

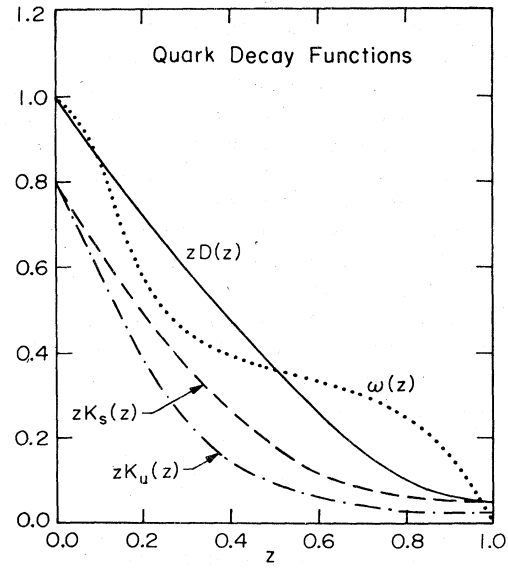


FIG. 8. Quark decay functions versus z where $D(z) \equiv D_u^{h^+}(z) + D_u^{h^-}(z)$, $K_s(z) \equiv D_s^{h^+}(z) + D_s^{h^-}(z)$, and $K_u(z) \equiv D_u^{K^+}(z) + D_u^{K^-}(z)$. Also shown is the function $\omega(z) \equiv D_u^{h^+}(z)/D_u^{h^+}(z)$, which was determined in Fig. 5(a).

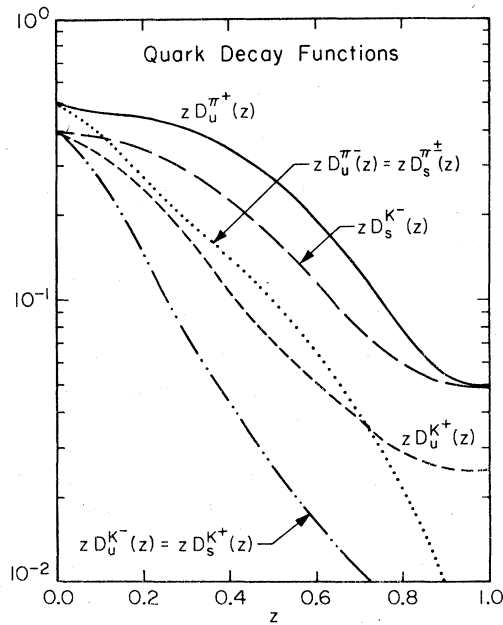


FIG. 9. The quark decay functions $zD_q^h(z)$ versus z . These functions are calculated from Fig. 8 and Table I.

tions.

The $D(z)$, $\omega(z)$, $K_s(z)$, and $K_u(z)$ functions are illustrated in Fig. 8 and the individual decay functions $D_q^h(z)$ arrived at from Table I are shown in Fig. 9. Table II gives the total percentage of momentum carried by the various mesons when decaying from a parent quark. For example, pions carry 63% of the momentum of a u quark and 45% of the momentum of an s quark.

It must be emphasized that our determination of these decay functions is very crude. We have combined our theoretical guesses with existing incomplete data to deduce $D_q^h(z)$. As the data improve (in particular, in separating π 's, K 's, and protons), one will be able to determine the behavior of these functions more precisely.

This completes our determination of the $G_{h-a}(x)$ and $D_q^h(z)$ functions entirely from lepton data [except for $G_{\pi^+ - a}(x)$ and the choice of K_s/K_u ratio as $z \rightarrow 1$, Eq. (3.10)]. We now turn to discuss the quark scattering function $d\hat{\sigma}(\hat{s}, \hat{t})/d\hat{t}$ for which hadron data themselves must be used, in combination with the G_{h-a} and D_q^h functions.

$$Ed\sigma/d^3p(s, t, u; A + B \rightarrow h + X) = \int_{x_a^{\min}}^1 dx_a \int_{x_b^{\min}}^1 dx_b G_{A-a}(x_a) G_{B-b}(x_b) D_c^h(z_c) \frac{1}{z_c} \frac{1}{\pi} \frac{d\hat{\sigma}}{d\hat{t}}(\hat{s}, \hat{t}; q_a + q_b - q'_a + q'_b), \quad (4.1)$$

where \hat{s} , \hat{t} , \hat{u} are the usual invariants but are calculated for the two-body reaction

$$\begin{aligned} \hat{s} &= (p_a + p_b)^2 = x_a x_b s, \\ \hat{t} &= (p_a - p_c)^2 = x_a t / z_c, \end{aligned} \quad (4.2)$$

TABLE II. Percentage of momentum carried by the mesons when they decay from a parent quark as determined by our analysis.

Meson	Quark	u	d	s
π^+		27%	15%	15%
π^0		21%	21%	15%
π^-		15%	27%	15%
Total π		63%	63%	45%
K^+		13%	8%	8%
K^0		8%	13%	8%
K^-		8%	8%	19%
\bar{K}^0		8%	8%	19%
Total K		37%	37%	54%
Total charged		63%	58%	57%
Total		100%	100%	99%

IV. THE QUARK-QUARK SCATTERING CROSS SECTION

$$d\hat{\sigma}/d\hat{t}(\hat{s}, \hat{t})$$

A. Formalism for large- p_\perp hadron-hadron collisions

All constituent or "hard-scattering" models which have been proposed to describe the hadron process $A + B \rightarrow h + X$ at large transverse momentum have the common underlying structure illustrated in Fig. 1(c).³¹ In the hard-scattering models the large-transverse-momentum reaction is assumed to occur as the result of a single large-angle scattering $a + b \rightarrow c + d$ of constituents a and b , followed in general by the decay or fragmentation of c into the observed particle h . Particular models differ in the choice of the basic interaction [$d\hat{\sigma}/d\hat{t}(\hat{s}, \hat{t}; a + b \rightarrow c + d)$]. For quark elastic scattering this interaction is $q_a + q_b \rightarrow q'_a + q'_b$, where q is a quark.³²⁻³⁴ In the constituent-interchange model (CIM),³⁵ the underlying large-angle reaction involves quark-hadron scattering (e.g., $q + \pi \rightarrow q + \pi$), whereas in the quark-fusion model the dominant subprocess is $\bar{q}q \rightarrow$ meson + meson.³⁶ In the multi-peripheral-type models, the large-angle process involves only hadrons (e.g., $\pi + \pi \rightarrow \pi + \pi$).

The calculation of the invariant cross section corresponding to Fig. 1(c) is done according to [$s = (p_A + p_B)^2$, $t = (p_A - p_h)^2$, and $u = (p_B - p_h)^2$]

$$\hat{u} = (p_b - p_c)^2 = x_b u / z_c.$$

The quantities x_a and x_b are the fractional momentum carried by quarks q_a and q_b , respectively, and the z_c is the fraction of the outgoing quark momen-

tum q_c that appears in the hadron. The two-to-two scattering constraint ($\hat{s} + \hat{t} + \hat{u} \approx 0$) implies

$$z_c = \frac{x_2}{x_b} + \frac{x_1}{x_a}, \quad (4.3)$$

where

$$\begin{aligned} x_1 &= -u/s = \frac{1}{2}x_\perp \cot \frac{1}{2}\theta_{c.m.}, \\ x_2 &= -t/s = \frac{1}{2}x_\perp \tan \frac{1}{2}\theta_{c.m.}, \end{aligned} \quad (4.4)$$

where $\theta_{c.m.}$ is the center-of-mass scattering angle and x_\perp is $2\sqrt{tu}/s$ (it is the momentum of h transverse to the direction of the incident hadrons A, B divided by the maximum possible, $\sqrt{s}/2$). The limits of integration in (4.1) are determined such that x_a , x_b , and z_c are between 0 and 1, namely

$$x_a^{\min} = x_\perp \cot \frac{1}{2}\theta_{c.m.} / (2 - x_\perp \tan \frac{1}{2}\theta_{c.m.}), \quad (4.5a)$$

$$x_b^{\min} = x_a x_\perp \tan \frac{1}{2}\theta_{c.m.} / (2x_a - x_\perp \cot \frac{1}{2}\theta_{c.m.}). \quad (4.5b)$$

The functions $G_{A-a}(x_a)$ represent the probability for the constituent a of particle A to have fractional longitudinal momentum x_a (see Secs. II A and B) and $D_c^h(z_c)$ is the probability that the constituent c fragments into a hadron (h) with fractional momentum $z_c = p_h/p_c$ (see Sec. III).

When calculating the contributions to $E d\sigma/d^3p$ from quark elastic scattering, we have assumed that all elastic quark-quark processes have amplitudes independent of quark color and flavor. That is, we take $d\hat{\sigma}/d\hat{t}(uu - uu) = d\hat{\sigma}/d\hat{t}(ud - ud) = d\hat{\sigma}/d\hat{t}(dd - dd) = d\hat{\sigma}/d\hat{t}(\bar{u}u - \bar{u}u)$, etc. We, of course, add the contributions to the scattering for the case where the fragmenting quark came from the beam to the case where the fragmenting quark came from the target (with the appropriate interchange of \hat{t} and \hat{u}).

Strictly speaking, the scattering for like-flavored quarks (e.g., uu) and unlike-flavored quarks (e.g., ud) are not exactly equal, even if the amplitudes are not flavor dependent. The difference arises from interference terms in the crossed diagram corresponding to particle exchange. These terms are largest for 90° quark scattering, but are reduced by color effects. The exact size and sign cannot be determined without knowing more about the character of the scattering, in particular the color-exchange properties.³⁷ Because of the smallness and uncertainty of these effects, we have left them out. In any case where interference terms have some effect such as in π^+/π^- ratios, the effects are usually overwhelmed by uncertainties in our input functions.

There is, however, one place where interference terms could be detected because they produce a small effect which would otherwise be exactly zero (assuming no other mechanism but that quark elastic scattering is affecting the data). The cross

sections for the production of π^0 mesons at say 90° from π^+ or π^- beams on protons are exactly equal in our model if there is no interference term. The asymmetry,

$$\alpha = \frac{\sigma(\pi^+p \rightarrow \pi^0X)}{\sigma(\pi^-p \rightarrow \pi^0X)} - 1$$

is a measure of the interference term. For example, suppose we are at such a large x_\perp that the proton is pure u quark; the scattering with a π^+ beam (ud) produces a different result from a π^- beam ($\bar{u}d$) because the former is affected by interference in the like-flavored (uu) scattering (half the time). We see in α the relative strength of the interference term in uu scattering, reduced by a factor which approaches $\frac{1}{2}$ at high x_\perp .

There should also be an annihilation diagram obtained from crossing quark-antiquark scattering, but an estimate shows that the term makes only a very small contribution to the total invariant cross section, so we have omitted it [thereby avoiding the decision of precisely how our empirical choices for $d\hat{\sigma}/d\hat{t}$ (4.8) are to be continued into the crossed region, $\hat{t} \rightarrow \hat{s}$].

The quarks in the hadrons as well as the hadrons from the fragmenting quark do have transverse momenta of mean value probably about 0.35 GeV. These do not seriously affect the considerations for this paper, and Eq. (4.1), which neglects them, will suffice. They are important for experiments involving correlations in momentum of particles of large p_\perp on opposite sides of the trigger hadron. In a later paper where we discuss such matters we shall take them into account and modify Eq. (4.1) appropriately.

B. Determination of $d\hat{\sigma}/d\hat{t}$

Suppose that the differential cross section for quark elastic scattering behaves at large \hat{s} and \hat{t} like

$$d\hat{\sigma}/d\hat{t} \sim \hat{s}^{-N} f(\hat{t}/\hat{s}), \quad (4.6)$$

that is, a homogeneous function of energy² of dimension N . Then Eq. (4.1) yields an invariant cross section for $A + B \rightarrow h + X$ of the asymptotic form

$$E d\sigma/d^3p(s, t, u; A + B \rightarrow h + X) = I(x_\perp, \theta_{c.m.}) [p_\perp^2]^{-N}. \quad (4.7)$$

As we discuss in more detail in Sec. V A, data on single-meson production at ISR and Fermilab do seem to scale in this way and to give $N \approx 4$. For simplicity we take N precisely equal to 4. In particular, we investigate the following possibilities for $d\hat{\sigma}/d\hat{t}$:

$$\frac{\hat{s}^2 + \hat{u}^2}{\hat{s}^2} \frac{1}{(-\hat{t})^4}, \quad (4.8a)$$

$$\frac{1}{\hat{s}} \frac{1}{(-\hat{t})^3}, \quad (4.8b)$$

$$\frac{1}{\hat{s}^2} \frac{1}{(-\hat{t})^2}, \quad (4.8c)$$

$$\frac{1}{\hat{s}^4}. \quad (4.8d)$$

The first form, (4.8a), is motivated by vector exchange with a form factor $F(t)$ which yields $[(\hat{s}^2 + \hat{u}^2)/\hat{s}^2 \hat{t}^2] F^2(\hat{t})$.³⁸

The remaining possibilities are phenomenological and are listed in order of decreasing dependence on \hat{t} . Form (4.8a) is the most peripheral (i.e., little \hat{s} dependence and strong \hat{t} dependence), whereas form (4.8d) is not peripheral at all (no \hat{t} dependence). The actual quark-quark scattering forces may not be as simple as any of these forms. It may contain logarithms or more complicated functions that change the power of p_\perp as a function of p_\perp and the power may not be an integer. However, at present we resist the use of more complicated quark-quark cross sections and hope that one of the above forms will give an adequate representation of the true cross section over the range of the data. Having fixed N we have only the degree of peripherality and the absolute normalization of $d\hat{\sigma}/d\hat{t}$ to determine.

Unfortunately there is no simple way to reduce data so that the function $f(\hat{t}/\hat{s})$ in (4.6) can be directly evaluated (as N was). It determines the angular distribution of the large- p_\perp hadrons, but in a way which is inextricably mixed with our assumptions concerning the quark distributions $G_{A-q}(x)$ and decay functions $D_q^n(z)$. With this understanding, however, we may attempt to distinguish among the forms (4.8a)–(4.8d) by comparing full calculations using our chosen G and D functions to experiment. This we do in the next section.

1. Angular dependence (x_\parallel dependence)

Figure 10 shows the $\theta_{c.m.}$ dependence of the invariant cross section for $p\bar{p} \rightarrow \pi^+ + X$ at $W = 53$ GeV and $p_\perp = 2.0$ and 3.3 GeV determined experimentally. Also shown are the $\theta_{c.m.}$ dependences resulting from quark-quark scattering cross sections of the forms (4.8a)–(4.8d), all normalized to agree at 90° and $p_\perp = 2.0$ GeV/c.

The ISR data³⁹ indicate that $E d\sigma/d^3 p$ is roughly constant for $40^\circ \leq \theta_{c.m.} \leq 90^\circ$ and $0 \leq p_\perp \leq 5.0$ GeV. This angular dependence disfavors scattering of the type (4.8a). This extremely peripheral form $(\hat{s}^2 + \hat{u}^2)/(\hat{s}^2 \hat{t}^4)$ results in a peaking of the invariant cross section away from 90° .

Another completely equivalent way of viewing the

$\theta_{c.m.}$ dependence is to plot the data at fixed energy and p_\perp versus x_\parallel as is done in Fig. 11. As was seen in Fig. 10 the x_\parallel dependence of the data favors $1/(-\hat{s}\hat{t}^3)$, but the form $1/(\hat{s}^2 \hat{t}^2)$ cannot be ruled out.

In this figure we have included some data at large x_\parallel .⁴⁰ For $x_\parallel \geq 0.7$ we are unsure whether the "spill-over" (as described in the Introduction) from the plateau region via e^{-6p_\perp} might not seriously affect the number of π^+ at p_\perp of only 2 GeV. (For $x_\parallel \geq 0.7$ the number of protons from the leading particle effect is already over 30 times the number of π^+ represented by the plotted point.) For definiteness we take $1/(-\hat{s}\hat{t}^3)$ for the remainder of this paper.

2. Radial scaling

Taylor *et al.*⁴¹ have observed that data on $p\bar{p} \rightarrow \pi^0 X$ are roughly independent of energy over the Fermilab and ISR range when plotted at fixed p_\perp and x_R ($x_R^2 = x_\parallel^2 + x_\perp^2$). In a hard-scattering approach radial scaling cannot be an exact principle of nature, since varying the energy at fixed x_R and

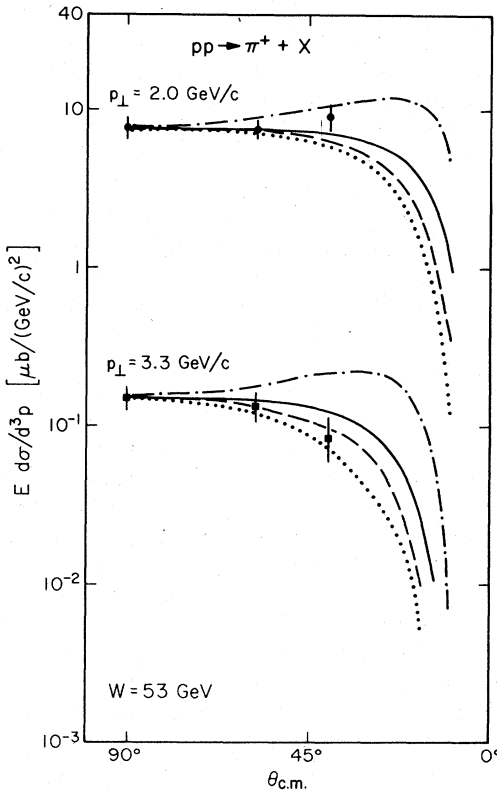


FIG. 10. The angular dependence of the invariant cross section $E d\sigma/d^3 p (p\bar{p} \rightarrow \pi^+ X)$ at $W = 53$ GeV and $p_\perp = 2.0$ and 3.3 GeV/c resulting from several choices for the quark-quark scattering differential cross section $d\hat{\sigma}/d\hat{t}$: $(\hat{s}^2 + \hat{u}^2)/(\hat{s}^2 \hat{t}^4)$ (dash-dot), $1/(-\hat{s}\hat{t}^3)$ (solid), $1/(\hat{s}^2 \hat{t}^2)$ (dashed), $1/\hat{s}^4$ (dotted). The data are from Ref. 39.

p_\perp changes both the integrand and the limits of integration in Eq. (4.1). Radial scaling requires a delicate balance between the angular dependence of $d\hat{\sigma}/d\hat{t}$ and the behavior of the structure $G_{p+q}(x)$ and the decay distributions $D_q^h(z)$. However, as can be seen from Fig. 12, the two quark-quark scattering forms, (4.8b) and (4.8c), favored by the $\theta_{c.m.}$ dependence at fixed p_\perp and fixed energy (Fig. 10) do exhibit approximate radial scaling. The form $1/(-\hat{s}\hat{t}^3)$ increases slightly with energy at fixed x_R while the form $1/(\hat{s}^2\hat{t}^2)$ decreases slightly.⁴²

3. Normalization

The normalized form for the quark-quark differential cross section used in the remainder of this paper is

$$d\hat{\sigma}/d\hat{t}(\hat{s}, \hat{t}; q_a + q_b \rightarrow q'_a + q'_b) = A/(-\hat{s}\hat{t}^3), \quad (4.9)$$

when q'_a is assumed to fragment into the observed hadron h and where,

$$A = 2.3 \times 10^6 \mu b \text{ GeV}^6. \quad (4.10)$$

The contribution of q'_b fragmentation into the observed hadron is calculated from (4.9) with \hat{t} and

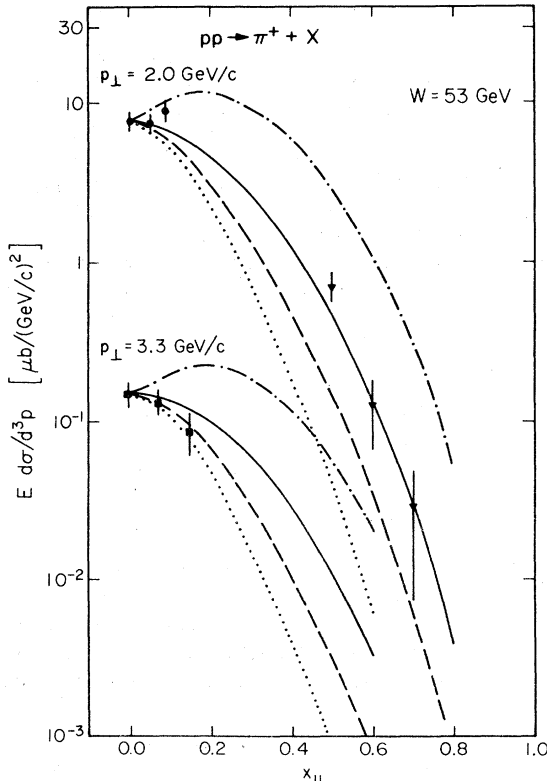


FIG. 11. Replot of Fig. 10 versus x_{11} instead of $\theta_{c.m.}$. The data at $p_\perp = 2.0 \text{ GeV}/c$ from Ref. 40 have been included (solid triangles).

\hat{u} interchanged.

In Eq. (4.9) the initial quarks q_a and q_b are averaged over color whereas the final quarks q'_a and q'_b are summed over color. We have assumed that the scattering is independent of the color of the individual quarks—with this definition, Eq. (4.9) is the same whether or not quarks have color.

The normalization A [(4.10)] was determined by comparing with the data of Fig. 13. The curves in this figure are predicted from the quark elastic scattering cross section (4.9) with A given by (4.10) (a one parameter fit). The agreement with the data for $p_\perp > 2.0 \text{ GeV}/c$ is excellent. Below $p_\perp = 2.0 \text{ GeV}/c$ the asymptotic form (4.9) results in an invariant cross section that rises (as p_\perp decreases) above the data and is in fact infinite at $p_\perp = 0$. Clearly this form should not be extrapolated to such small p_\perp values, where mass effects must alter the form in such a way as to decrease the result. Because we do not know how to represent these mass effects properly and because for p_\perp small the non-hard-scattering “plateau” term is becoming dominant anyway, we only consider the region of p_\perp greater than $2.0 \text{ GeV}/c$.

At first sight the normalization A may look very large, for one expects normal cross sections of a few tenths of an mb at GeV ranges of energy. However, in a qq collision at 90° with $\hat{p}_\perp = 2 \text{ GeV}$ (below which we do not expect our formulas to be valid) each quark has 2 GeV in the c.m. frame ($\hat{s} = 16 \text{ GeV}^2$, $\hat{t} = 8 \text{ GeV}^2$) and Eq. (4.9) gives $d\hat{\sigma}/d\hat{t}$ of $0.28 \text{ mb}/(\text{GeV})^2$. For larger \hat{s} , \hat{t} it falls rapidly.

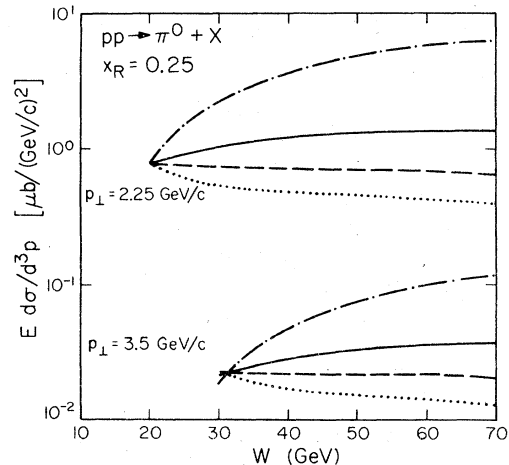


FIG. 12. Radial scaling implies a cross section independent of energy at fixed p_\perp and x_R ($x_R = x_1/\sin\theta_{c.m.}$). This turns out to be approximately true for $pp \rightarrow \pi^0 + X$ for our model with $d\hat{\sigma}/d\hat{t} \propto 1/(-\hat{s}\hat{t}^3)$. In this figure the same information as in Fig. 10 is plotted in still another form, the energy dependence ($W = \sqrt{s}$) of the invariant cross section $E d\sigma/d^3p$ ($pp \rightarrow \pi^0 + X$) at fixed p_\perp and $x_R = 0.25$.

As is well known, dimensional analysis⁴³ of field theory with any finite number of diagrams predicts a quark-quark scattering which gives a $1/p_{\perp}^4$ behavior of the single-particle invariant cross section. It is interesting to compare the size of the cross section (4.9) with a typical $1/p_{\perp}^4$ contribution to see, in particular, at what p_{\perp} one might expect the latter term to dominate over the former with a given coupling constant. As an example consider the quark-quark scattering cross section expected in first-order perturbation theory from the exchange of one color octet of vector gluons by colored quarks. This is

$$d\hat{\sigma}/d\hat{t} = 2\pi(8/9)f^4(\hat{s}^2 + \hat{u}^2)/\hat{s}^2\hat{t}^2, \quad (4.11)$$

where f^2 is the coupling constant. This cross section is equal to (4.9) at $\hat{\theta}=90^\circ$ ($\hat{t}=\hat{u}=-\hat{s}/2$) if

$$f^2 = 41 \text{ GeV}^2/\hat{s}. \quad (4.12)$$

The theory of asymptotic freedom yields⁴⁴

$$f^2 = 4\pi/(9 \ln Q^2/\Lambda^2), \quad (4.13)$$

when the quarks are off their mass shell and Q is a typical momentum transfer. In our case the quarks are nearly on the mass shell so that we do not know if (4.13) is applicable; nevertheless, as an exercise we use (4.13) with Q^2 replaced by $-\hat{t}$. For $\Lambda=0.5$ GeV (see Ref. 45) this results in an expected f^2 of about 0.25 at energies around $W=53$ GeV, $p_{\perp}=6$ GeV/c ($\hat{s}=140$ GeV 2), which is about as high a value of \hat{s} for which we have tested the scattering with data in this paper. This is comparable with (4.12) at this \hat{s} value ($f^2 \approx 0.3$) so such a scattering (varying as p_{\perp}^{-4}) might still be lurking below the scattering (varying as p_{\perp}^{-8}) that we are observing and analyzing here. We are therefore not yet in direct contradiction to (4.13) [further the quantum-chromodynamic model implies additional logarithmic modifications of the structure functions $G_{h \rightarrow q}(x)$ which reduces the scattering a bit more]. It is of profound experimental interest to continue to push to higher p_{\perp} to test whether the scattering continues to scale as p_{\perp}^{-8} , or eventually a p_{\perp}^{-4} term begins to appear. We continue to analyze with our empirical formula (4.9).

V. PREDICTIONS OF THE QUARK ELASTIC SCATTERING MODEL

A. Energy dependence at fixed p_{\perp} (x_{\perp} dependence)

The dependence of $E d\sigma/d^3p$ on energy at fixed p_{\perp} and $\theta_{\text{c.m.}}$ resulting from quark elastic scattering is not sensitive to the detailed form for $d\hat{\sigma}/d\hat{t}$ (see Table III). The x_{\perp} dependence of [see Eq. (4.7)]

$$I(x_{\perp}, \theta_{\text{c.m.}}) = p_{\perp}^{2N}(E d\sigma/d^3p) \quad (5.1)$$

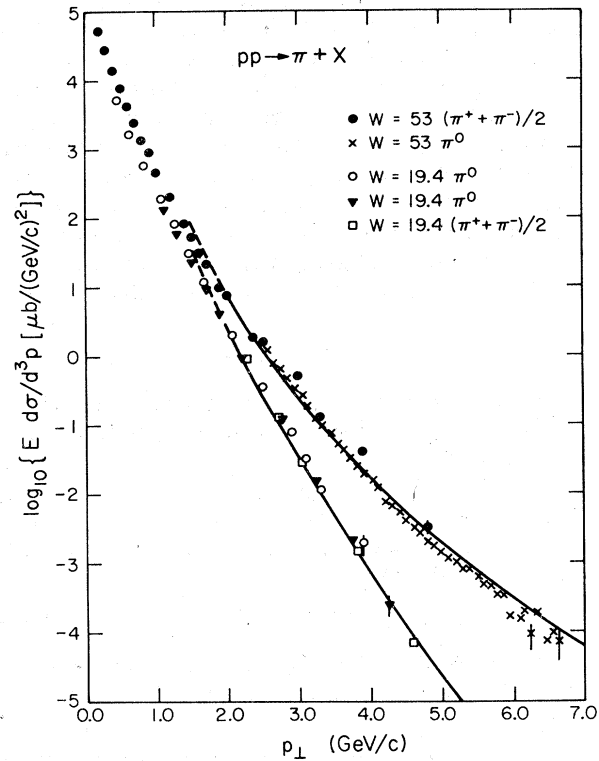


FIG. 13. Experimental behavior of $E d\sigma/d^3p (pp \rightarrow \pi^+ + X)$ at 90° versus p_{\perp} for $W=19.4$ and 53 GeV ($W=\sqrt{s}$) [we plot $\log_{10}(E d\sigma/d^3p)$]. The data are $pp \rightarrow \pi^0 + X$ from Ref. 47 (crosses), D. C. Carey *et al.* [Phys. Rev. D **14**, 1196 (1976); D. C. Carey *et al.*, Fermilab Report No. Fermilab-Pub-75/20-EXP, 1975 (unpublished)] (open circles), Ref. 49 (solid triangles), $pp \rightarrow (\pi^+ + \pi^-)/2 + X$ from Ref. 39 (solid circles), and $pN \rightarrow (\pi^+ + \pi^-)/2 + X$ from J. W. Cronin *et al.* (Chicago-Princeton collaboration) [Phys. Rev. D **11**, 3105 (1975); see Ref. 52] (open squares). The solid curves are the prediction of our model with $d\sigma/dt = A/(-st^3)$. The agreement in shape is a test of the model, whereas the normalization A is chosen to fit the data. Our results should not be extrapolated below $p_{\perp}=2.0$ GeV/c, where the simple form chosen for $d\hat{\sigma}/d\hat{t}$ produces an invariant cross section that rises to infinity as p_{\perp} decreases to zero (dashed curve).

is determined primarily by the behavior of the structure and decay functions $G_{p \rightarrow q}(x)$ and $D_q^R(z)$, respectively. Our homogeneity assumption implies that multiplying the invariant cross section by p_{\perp}^{2N} should yield a universal function of x_{\perp} and $\theta_{\text{c.m.}}$.

The experimental situation is a bit unclear. All experiments on π production at 90° seem to scale (function of x_{\perp} only) when multiplied by p_{\perp}^{2N} , but each experiment quotes differing values of N ranging from $2N=7.2$ (Ref. 46) to $2N=8.6$ (Ref. 47). Presumably these discrepancies are due to

TABLE III. Experimental observations that depend strongly (weakly) on the details of the choice of the quark-quark scattering differential cross section $d\hat{\sigma}/d\hat{t}$. (Note: $W = \sqrt{s}$, $x_1 = 2p_\perp/W$, $x_R = x_1/\sin\theta_{c.m.}$).

Strongly dependent	Weakly dependent
(a) $E d\sigma/d^3p$ vs p_\perp at fixed W and fixed $\theta_{c.m.}$	(a) $E d\sigma/d^3p$ vs W at fixed p_\perp and fixed $\theta_{c.m.}$ (i.e., x_1 dependence)
(b) $E d\sigma/d^3p$ vs x_1 (or $\theta_{c.m.}$) at fixed W and p_\perp	(b) Beam ratios vs x_1 (should not depend on W) at fixed $\theta_{c.m.}$ [e.g., $\sigma(pp \rightarrow \pi^0 X)/\sigma(\pi p \rightarrow \pi^0 X)$]
(c) $E d\sigma/d^3p$ vs W at fixed x_R and p_\perp	(c) Detected particle ratios vs x_1 (should not depend on W) at fixed $\theta_{c.m.}$ [e.g., $pp \rightarrow (\pi^+/\pi^-) + X$ $pn \rightarrow (\pi^+/\pi^-) + X$, etc.]
	(d) Target ratios vs x_1 (should not depend on W) at fixed $\theta_{c.m.}$ [e.g., $\sigma(pp \rightarrow \pi^0 X)/\sigma(pn \rightarrow \pi^0 X)$]

the experimental difficulties in measuring such small cross sections. Having chosen $N = 4$ for simplicity, we compare in Fig. 14 most of the existing data (at 90°) on π production multiplied by p_\perp^{-8} with our predicted scaling function $I(x_1, \theta_{c.m.} = 90^\circ)$. Clearly, even if we were to allow for large errors in the experimental normalizations, it is not possible to simultaneously fit all experiments. They are inconsistent with one another. Nevertheless, it can be seen that the predicted x_1 dependence does agree with the overall trend of the data. The rise with energy from Fermilab ($x_1 \approx 0.7$) to ISR ($x_1 \approx 0.1$) is correctly predicted (see also Fig. 13). Considering that this x_1 dependence is predicted from data on electron and neutrino processes we view the agreement as good.⁴⁸

For completeness, in Fig. 15 we display the predicted $I(x_1, \theta_{c.m.})$ scaling function for $pp \rightarrow \pi^0 + X$ at 90° and 45°. In addition, we show the individual contributions at 90° from elastic scattering of quarks of various flavors (e.g., $uu \rightarrow uu$, $dd \rightarrow dd$, $ud \rightarrow ud$, etc.).

B. The beam ratio $\sigma(pp \rightarrow \pi^0 X)/\sigma(\pi p \rightarrow \pi^0 X)$

One important way to investigate the constituent (or quark) nature of hadrons is to compare the large- p_\perp invariant cross sections for $pp \rightarrow \pi^0 X$ and $\pi^\pm p \rightarrow \pi^0 X$. The quark-elastic-scattering model predicts definite differences in these processes owing to the different quark distributions within the proton and the pion of the beam. The \hat{s}^{-N} scaling, Eq. (4.6), means that the ratio $\sigma(pp \rightarrow \pi^0 X)/\sigma(\pi p \rightarrow \pi^0 X)$ is independent of p_\perp , and hence energy, and depends only on x_1 and $\theta_{c.m.}$. Figure 16 shows the recent data from a Caltech-BNL-LBL⁴⁹ collaboration which do appear to scale in x_1 .

In order to predict this beam ratio we must know the quark distributions within the pion. These are discussed in Sec. II B. There is no experimental information concerning these distributions, so as a first guess we assume that $xu^{\pi^+}(x) [=xd^{\pi^+}(x)]$ is a constant ($C = 0.25$) for all x and

neglect contributions from nonvalence quarks. This yields a prediction for $\sigma(pp \rightarrow \pi^0 X)/\sigma(\pi p \rightarrow \pi^0 X)$ shown in Fig. 16 by the dashed curve.

Obviously we really do not know the quark distributions within the pion. Now that we have data on the beam ratio we can construct the slightly more sophisticated pion structure functions shown in Fig. 4(b). The beam ratio is expected from these pion quark distributions is shown by the solid curve in Fig. 16.⁵⁰ We shall hereafter use these quark distributions for pions for all further predictions.

The data (of Fig. 16) probably exclude models which require that both the quark and the antiquark in the outgoing pion are required to come from the incident hadrons. This, of course, because the proton can supply so few antiquarks whereas the pion has a valence antiquark. For comparison, we have estimated the beam ratio $\sigma(pp \rightarrow \pi^0 X)/\sigma(\pi p \rightarrow \pi^0 X)$ that would arise if only the annihilation piece of the process $\bar{q}q \rightarrow \bar{q}q$ made up the total single-particle cross section. This term is small in our model and we have neglected it. Nevertheless, to illustrate a point we estimate the beam ratio resulting from such a process. This term is calculated using $d\hat{\sigma}/d\hat{t}(\bar{q}q \rightarrow \bar{q}q, \text{annihilation}) = -A\hat{t}/\hat{s}^5$, which is obtained by crossing the elastic term $qq \rightarrow qq$ [(4.9)]. This procedure is extremely naive and cannot be trusted for the magnitude of the annihilation term; however, the detailed form for $d\hat{\sigma}/d\hat{t}(\bar{q}q \rightarrow \bar{q}q, \text{annihilation})$ is relatively unimportant in determining the beam ratio. The results are shown by the dotted curve in Fig. 16 and are clearly much smaller than the data. This implies that quark-antiquark processes can only make up a relatively small contribution to the total single-particle cross section in pp collisions for $x_1 \gtrsim 0.3$.⁵¹

A sharp test of the quark-quark scattering approach is the prediction that as one probes the beam particle closer to $x_a = 1$ the ratio $\sigma(\pi p \rightarrow \pi^0 X)/\sigma(pp \rightarrow \pi^0 X)$ should rise strikingly. The pion-in-

itiated process [$x u \pi^+(x) \sim \text{const}$] will dominate over the proton-initiated one [$x u(x) \sim (1-x)^3$]. Figure 17 shows that at $\theta_{\text{c.m.}} = 90^\circ$ and $x_\perp = 0.35$ the mean

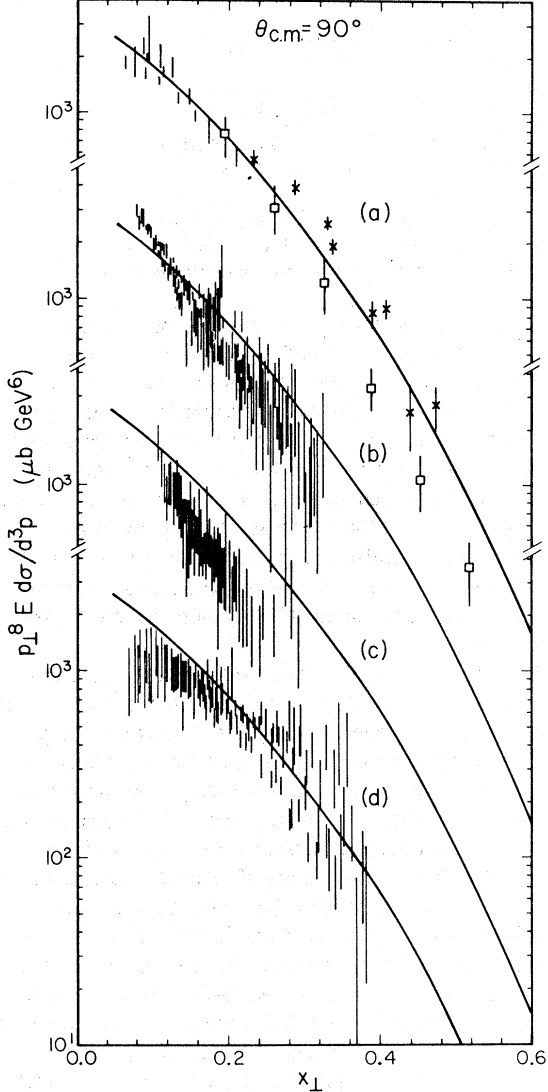


FIG. 14. Attempt to test experimentally the question of whether data at 90° scales as $1/p_\perp^8$. Comparison of $I(x_\perp, 90^\circ) = p_\perp^8 E d\sigma/d^3p$ from our model to data from various sources: (a) $p\bar{p} \rightarrow (\pi^+ + \pi^-)/2 + X$ for $W = 23, 31, 45, 53$, and 63 GeV from Ref. 39 (vertical lines), $pN \rightarrow (\pi^+ + \pi^-)/2 + X$ for $W = 23.7$ GeV from Cronin *et al.* (see caption of Fig. 13) (open squares), $p\bar{p} \rightarrow \pi^0 + X$ for $W = 13.7$ and 19.4 GeV from Ref. 49 (crosses). (b) $p\bar{p} \rightarrow \pi^0 + X$ for $W = 23, 31, 45, 53$, and 63 GeV from Ref. 47 (vertical lines). (c) $p\bar{p} \rightarrow (\pi^+ + \pi^-)/2 + X$ for $W = 45, 53$, and 63 GeV from Ref. 47 (vertical lines). (d) $p\bar{p} \rightarrow \pi^0 + X$ for $W = 23, 31, 45, 53$, and 63 GeV from Ref. 46 (vertical lines). In all cases the theoretical curve is the same, and it is evident that data from different references even at the same energy are not mutually consistent. Also, it is clear that the data in (c) could be re-normalized to agree with our prediction.

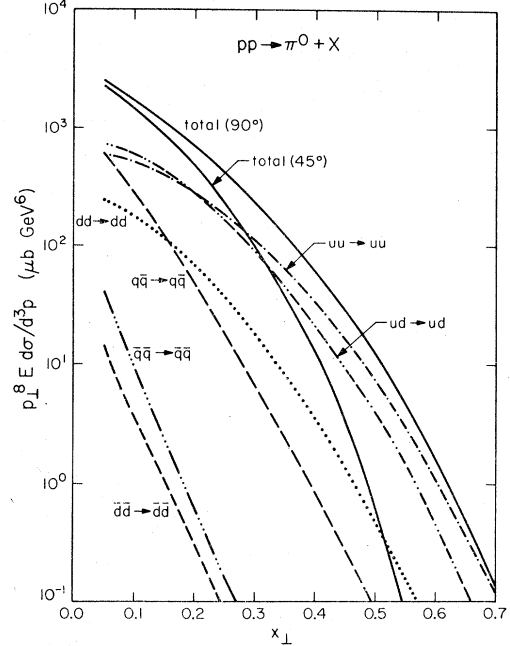


FIG. 15. The theoretical x_\perp dependence of $I(x_\perp, \theta) = p_\perp^8 E d\sigma/d^3p$ ($p\bar{p} \rightarrow \pi^0 + X$) at 90° and 45° according to the quark-elastic-scattering model. Also shown are the contributions to $I(x_\perp, 90^\circ)$ that arise from various flavors of quarks elastically scattering: $uu \rightarrow uu$, $dd \rightarrow dd$, $ud \rightarrow ud$ (actually $ud \rightarrow ud + du \rightarrow du$), $q\bar{q} \rightarrow q\bar{q}$ (actually $q\bar{q} \rightarrow q\bar{q} + \bar{q}\bar{q} \rightarrow \bar{q}q$, where q is the sum over u , d , and s), $\bar{q}\bar{q} \rightarrow \bar{q}\bar{q}$, and $d\bar{d} \rightarrow d\bar{d}$.

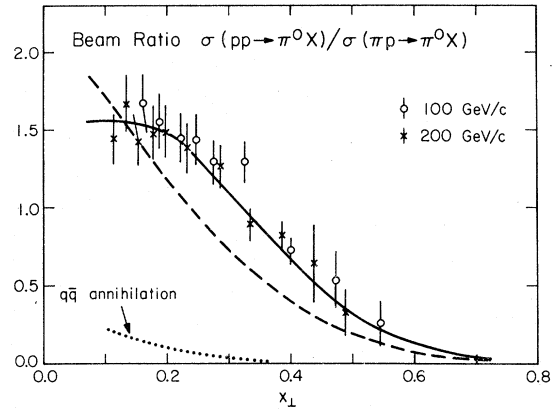


FIG. 16. Hadron data used to help determine the quark distributions within the pion [Fig. 4(b)]. The ratio of the invariant cross section $\sigma(p\bar{p} \rightarrow \pi^0 + X)/\sigma(\pi^+ p \rightarrow \pi^0 + X)$ at $\theta_{\text{c.m.}} = 90^\circ$ and $p_{\text{lab}} = 100$ and 200 GeV/c (Ref. 49). The model expects this ratio to depend only on x_\perp at fixed $\theta_{\text{c.m.}}$ in agreement with the data. The dashed curve is the prediction of the model using $xu\pi^+(x) = 0.25$ and $x\bar{u}\pi^+(x) = 0$. We adjust the quark distribution functions for the pion to those of Fig. 4(b) (solid curve) in order to achieve the agreement shown here by the solid curve. Also shown (dotted curve) is the predicted ratio from a quark-antiquark annihilation term, which is small because there are many more antiquarks with large x within a pion than within a proton.

value of $\langle x_a \rangle_{\text{beam}}$ sampled is only about 0.4. At 35° , on the other hand, $\langle x_a \rangle_{\text{beam}} \approx 0.7$ at this same x_\perp value. Thus at the same x_\perp we expect to see a rapid increase of $\sigma(\pi p \rightarrow \pi^0 X)/\sigma(pp \rightarrow \pi^0 X)$ as the c.m. angle changes from 90° to 35° . This is shown in Fig. 18.⁴⁹

Since, for our best choice of $d\hat{\sigma}/d\hat{t}$, the cross sections for $pp \rightarrow \pi^0 X$ and $\pi p \rightarrow \pi^0 X$ nearly scale in x_R , the ratio is nearly a function of x_R independent of $\theta_{\text{c.m.}}$ (for $90^\circ \leq \theta_{\text{c.m.}} \leq 35^\circ$). This is seen in Fig. 19, where we plot the same information as in Fig. 18 but in the variable $x_R = x_\perp/\sin\theta_{\text{c.m.}}$ instead of x_\perp . The ratio does not scale in x_R in the backward direction ($\theta_{\text{c.m.}} = 145^\circ$).

C. Particle ratios

1. $pN \rightarrow (\pi^+/\pi^-) + X$, $pp \rightarrow (\pi^+/\pi^-) + X$

Having determined the quark probability functions, $G_{N \rightarrow q}(x)$, and the decay distributions, $D_q^{\pi^+}(x)$,

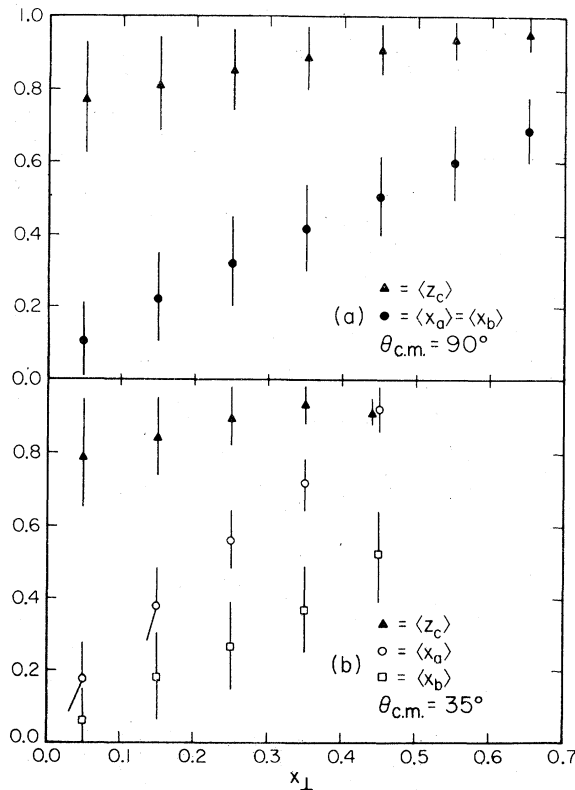


FIG. 17. The mean values of the fraction of momentum carried by the incoming quarks (x_a = beam, x_b = target) and the mean value of the fraction of momentum carried by the detected hadron of parent quark (z_c) from the quark-elastic-scattering model. (a) Mean values of x_a (solid dots) and z_c (solid triangles) at $\theta = 90^\circ$ from $pp \rightarrow \pi^0 + X$ versus x_\perp from the quark-elastic-scattering model (at $90^\circ \langle x_a \rangle = \langle x_b \rangle$). The error bars are not errors. They represent the standard deviation $\sigma(x^2 - \langle x \rangle^2)$ from the mean. (b) Same as (a) but at $\theta_{\text{c.m.}} = 35^\circ$. Here $\langle x_a \rangle$ (open circles) does not equal $\langle x_b \rangle$ (open squares).

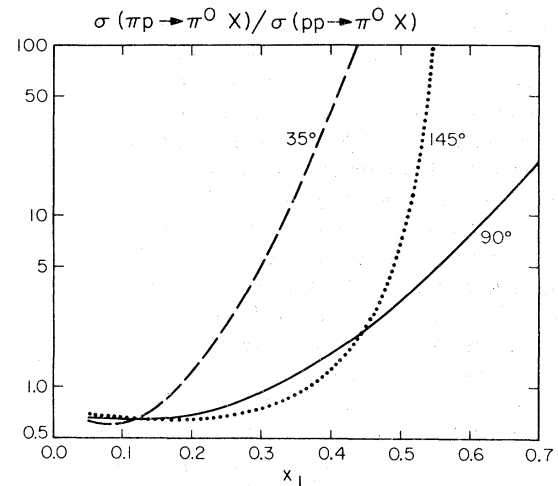


FIG. 18. Predictions for the ratio $\sigma(\pi p \rightarrow \pi^0 X)/\sigma(pp \rightarrow \pi^0 X)$ versus x_\perp at $\theta_{\text{c.m.}} = 90^\circ$, 35° , and 145° resulting from the quark-elastic-scattering model with $d\hat{\sigma}/d\hat{t} = A/(-\hat{s}\hat{t}^3)$. Our model (with no interference terms) predicts $\sigma(\pi^+ p \rightarrow \pi^0 X) = \sigma(\pi^- p \rightarrow \pi^0 X)$. The rapid variation of this ratio with $\theta_{\text{c.m.}}$ is due to the fact that as the scattering becomes more forward the values of $\langle x_a \rangle_{\text{beam}}$ sampled approach 1 [see Fig. 17(b)], where there is a greater difference between the pion structure function (~constant) and the proton structure function ($\sim(1-x)^3$).

and the form of the quark-quark scattering, $d\hat{\sigma}/d\hat{t}$, we can predict the π^+/π^- ratio at large p_\perp without any free parameters. In fact, this ratio is not sensitive to the detailed form of $d\hat{\sigma}/d\hat{t}$ (see Table III) and is thus excellent test of our underlying hypotheses.

Since u quarks dominate over d quarks in the proton as $x_a \rightarrow 1$ and since the u quark fragments predominantly into π^+ 's at large z values one would expect to see many more π^+ 's than π^- 's at large p_\perp . Experimentally this is not the case at ISR; this fact appears on the surface to be in

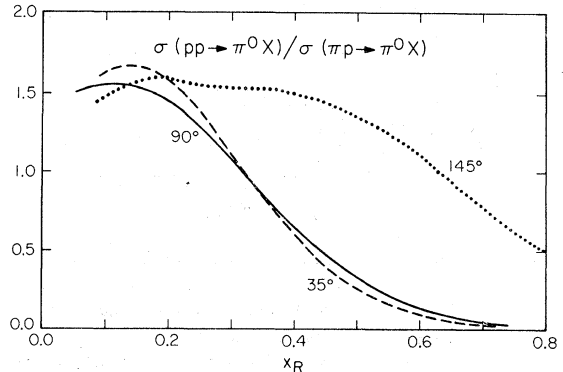


FIG. 19. The inverse of the same ratio as in Fig. 18, but plotted versus x_R ($x_R = x_\perp/\sin\theta_{\text{c.m.}}$). The rough radial scaling for $90^\circ \leq 35^\circ$ resulting from the model is clear.

disagreement with our approach. On the contrary, as can be seen in Fig. 20, predictions from our model are not in serious disagreement with the ISR data. The model predicts a π^+/π^- ratio of only about 1.25 at $p_\perp = 3.0 \text{ GeV}/c$ and $W = 53 \text{ GeV}$. This ratio is close to 1 for two reasons. Because we are at high energy ($W = 53 \text{ GeV}$), x_\perp is quite small and thus we are sampling the quark distributions within the protons at small x_a (and x_b) values (0.2 at $p_\perp = 3$, see Fig. 17) where there is not so much difference between the number of u and d quarks. Secondly, we are sampling the quark decay functions $D_q(z_c)$ in a region of z_c where there is a reasonable probability for an up-quark to fragment into a π^- . To see the expected large π^+/π^- ratio one must perform experiments in regions of larger x_\perp (i.e., large p_\perp at Fermilab energies). Unfortunately, this ratio has only been measured off nuclear targets at Fermilab (average over neutrons and protons). A nuclear target has roughly equal numbers of u and d quarks and at 90° both beam and target are of equal importance in determining the flavor of the fragmenting quark. Thus the π^+/π^- ratio is not expected to be nearly as large off such a target and our predictions yield $\pi^+/\pi^- \approx 1.6$ at $p_\perp = 5.0 \text{ GeV}/c$ and $p_{\text{lab}} \approx 200 \text{ GeV}/c$ in agreement with the $\theta_{\text{c.m.}} \approx 90^\circ$ at Fermilab data⁵² (Fig. 20). As can be seen from Fig. 21

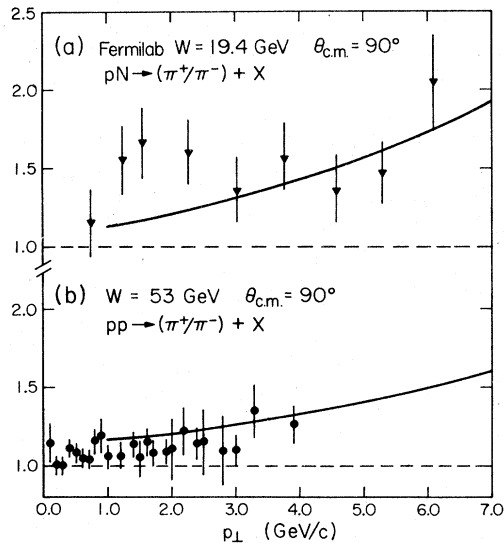


FIG. 20. Comparison of some of the particle ratio predictions of Fig. 21 with data. (a) $pN \rightarrow (\pi^+/\pi^-) + X$ at $W = 19.4 \text{ GeV}$ and $\theta_{\text{c.m.}} = 90^\circ$ compared with data from Cronin *et al.* (see caption of Fig. 13), where $N = (p+n)/2$ (see Ref. 52). (b) $pp \rightarrow (\pi^+/\pi^-) + X$ at $W = 53 \text{ GeV}$ and $\theta_{\text{c.m.}} = 90^\circ$ compared with data from Ref. 39. Below $p_\perp = 2 \text{ GeV}/c$ the soft-pion plateau (with $\pi^+/\pi^- = 1$) comes in to reduce the quark elastic scattering ratio eventually yielding a ratio of one at $p_\perp = 0$.

we predict the π^+/π^- ratio at 90° off protons to become large at high x_\perp . The ratio should be as large as 2 at $x_\perp \approx 0.4$ and even larger at higher x_\perp values. If π^+ production in pp collisions does not begin to dominate over π^- production at Fermilab energies and large p_\perp as predicted in Fig. 21, our approach (with quark but not gluon scattering) will be in *serious* trouble. We have no free parameters to vary. Our only freedom lies in the choice of $d\hat{\sigma}/d\hat{t}$ and the π^+/π^- ratios do not depend sensi-

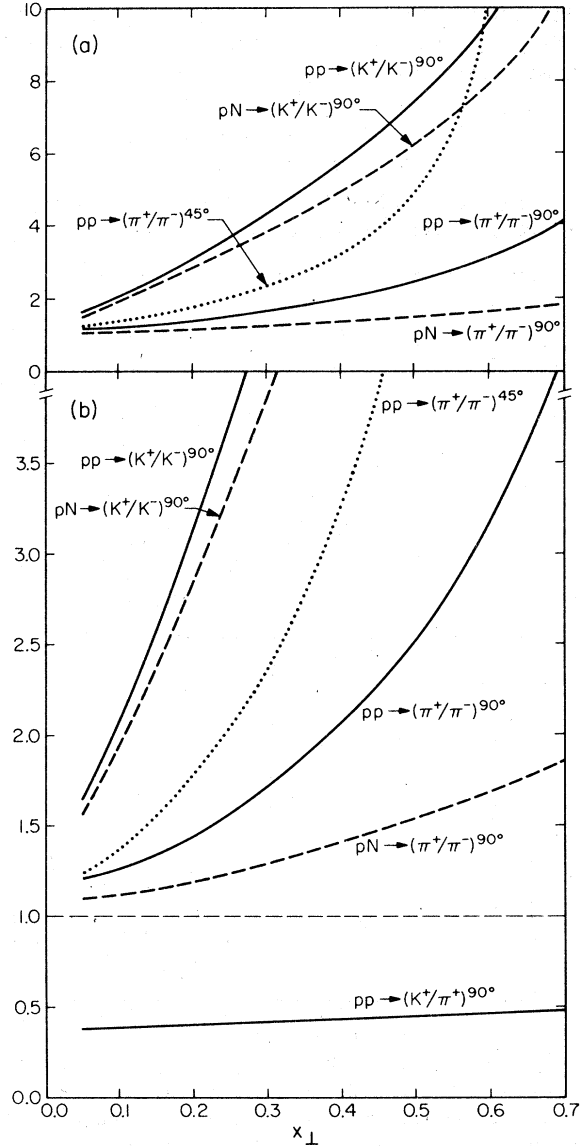


FIG. 21. Particle ratios predicted from the quark-elastic-scattering model. (a) $pp \rightarrow (\pi^+/\pi^-) + X$ at 90° and 45° , $pN \rightarrow (\pi^+/\pi^-) + X$ at 90° , and $pp \rightarrow (K^+/K^-) + X$ and $pN \rightarrow (K^+/K^-) + X$ at 90° , where N is the average of proton and neutron, $N = (p+n)/2$. (b) Same as (a) but with a different scale and where we have included the ratio $pp \rightarrow (K^+/\pi^+) + X$ at 90° .

tively on the precise form. They do depend on the assumed decay functions, in particular $\omega(z)$ (see Sec. III F), but this has been determined by neutrino data and rather strong theoretical arguments.⁵³

The angular dependence of the π^+/π^- ratio is another interesting test of the predictions. As was mentioned earlier when discussing beam ratios, one samples the beam particle closer to $x_a = 1$ at forward $\theta_{c.m.}$ angles than at 90° (see Fig. 17). In addition, in the more forward direction the beam quark is more likely to be the one producing the observed hadron (this is due to the peripheral nature of the quark-quark force). This results in a predicted π^+/π^- ratio off protons that is much larger at 45° than at 90° for the same x_\perp (see Fig. 21).⁵⁴

2. $pN \rightarrow (K^+/K^-) + X, pp \rightarrow (K^+/K^-) + X$

The rough estimates for the quark decay functions into kaons given in Table I and Fig. 9 allow us to predict the large p_\perp (K^+/K^-) ratios shown in Fig. 21. Because of the lack of kaon production data in lepton-initiated processes, we were forced to make crude assumptions concerning these decay probabilities. Consequently these predictions are not as accurate as those for pions. If our model ratios for pions are confirmed we can hope to use experimental data on K^+/K^- ratios to improve our knowledge of the decay functions $D_u^{K^+}$. Nevertheless, some features are reliably predicted. Because the u quark can fragment directly into a K^+ [via $K_u(z)$ in Table I], whereas a K^- must be produced either from an s or \bar{u} quark or indirectly through the function $\omega(z)$, we expect K^+/K^- to become large (in fact larger than π^+/π^-) as x_\perp increases toward 1. The data in Fig. 22 do substantiate this.⁵² In addition, we expect that the $90^\circ K^+/K^-$ ratio is slightly larger off protons than off the average $(n+p)/2$ as shown in Fig. 21.

3. $pN \rightarrow (K^+/\pi^+) + X, pp \rightarrow (K^+/\pi^+) + X$

The behavior of the ratio $pp \rightarrow K^+/\pi^+$ as x_\perp becomes large determines the behavior of $D_u^{K^+}(z)/D_u^{\pi^+}(z) = K_u(z)/D(z)$ as $z \rightarrow 1$ (see Table I and Sec. III C). The naive guess that $D(z)/K_u(z) = 1$ yields the dotted curve in Fig. 22(b), which is in disagreement with data. We have used the observation that $\sigma(pp \rightarrow K^+ + X)/\sigma(pp \rightarrow \pi^+ + X) \approx 0.5$ as x_\perp becomes large to determine that $K_u(z)/D(z) \approx 0.5$ at $z = 1$. Having determined this, we predict that there is little x_\perp dependence in the ratio K^+/π^+ (Fig. 21) in agreement with the data (Fig. 22).

The ratios π^+/π^- or K^+/K^- have striking variations with x_\perp or angle or beam particle, while

the ratio K^+/π^+ does not. This is because the former ratios depend so much on the quality u , and d of the quarks coming out with high p_\perp and these ratios depend on x_\perp through the variations of x_a, x_b and thus of $u(x_a)$ or $d(x_a)$, under different conditions. But for K^+/π^+ the ratio depends on the disintegration properties of the quark and is nearly the same for u or for d quarks. It measures the relative difficulty of getting new $s\bar{s}$ pairs in the cascade compared to $\bar{u}u$ pairs (or $\bar{d}d$ pairs). Apparently they are not equal as SU(3) would have it, but $\bar{s}s$ pairs are found only half as frequently as $\bar{u}u$.

4. $pp \rightarrow (\eta/\pi^0) + X$

To understand η/π^0 production ratios we shall have to guess at a new function $D_u^\eta(z)$ [equals $D_d^\eta(z)$]. For the high- p_\perp experiments, as we have pointed out before, only z near 1 is important. Figure 17 shows that the mean z in the range of data ($0.15 \leq x_\perp \leq 0.3$) is greater than 0.8, so we can suppose the original quark, say u , is com-

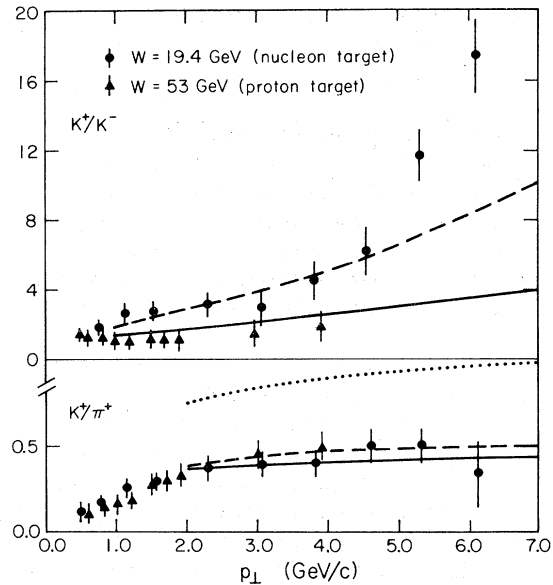


FIG. 22. Comparison of some of the particle-ratio predictions of Fig. 21 with data. (a) $pN \rightarrow (K^+/K^-) + X$ at $W = 19.4$ GeV (dashed curve) (Ref. 52) and $pp \rightarrow (K^+/K^-) + X$ at $W = 53$ GeV (solid curve) compared with the data of Cronin *et al.* (see caption of Fig. 13) and Ref. 39, respectively. (b) Data on the ratio $pN \rightarrow (K^+/\pi^+) + X$ at $W = 19.4$ GeV (Cronin *et al.*) (solid triangles) (Ref. 52) and on $pp \rightarrow (K^+/\pi^+) + X$ at $W = 53$ GeV (Ref. 39, solid dots). The dotted curve is the K^+/π^+ ratio at $W = 19.4$ GeV resulting if one assumes that $K_u(z) = K_s(z) = D(z)$ at $z = 1$ [exact SU(3)]. We used these data to determine one parameter—the relative ease of making new strange-quark pairs—resulting in the fits shown. The dashed (solid) curve is at $W = 19.4$ GeV (53 GeV) with the broken SU(3) solution [$K_u(z) < K_s(z)$] shown in Fig. 8.

bined with a new \bar{u} from a pair, just as it is for π^0 .

The quark contents of the π^0 and η are given by

$$\pi^0 = \frac{1}{\sqrt{2}} (u\bar{u} - d\bar{d}), \quad (5.2a)$$

$$\eta = \cos\theta_\eta (s\bar{s}) + \sin\theta_\eta \frac{1}{\sqrt{2}} (u\bar{u} + d\bar{d}). \quad (5.2b)$$

Hence near $z \rightarrow 1$, $D_q^\eta(z)/D_q^{\pi^0}(z) \rightarrow \sin^2\theta_\eta$ for any nonstrange quark q . We have neglected any effects due to η, π^0 mass differences in this decay. This is to be contrasted with the K^+/π^+ apparent "mass effect," which is not due to the extra mass of the K^+ so much as to the difficulty of making $s\bar{s}$ pairs because of the mass of the s quark. Given a u quark a K^+ must pick up an \bar{s} , but both η and π^0 only require a \bar{u} .

As z becomes smaller $D_q^\eta(z)/D_q^{\pi^0}(z)$ will fall because π^0 's come so much more easily than η 's as secondaries from various decays. The values of θ_η that are determined in various ways from the properties of the η according to the quark model lie between 45° and 58° with the smaller value somewhat favored.⁵⁵ This predicts an η/π^0 ratio at large p_\perp in the range

$$0.5 \leq (\eta/\pi^0) \leq 0.72, \quad (5.3)$$

with the lower number favored. Recent data from ISR⁴⁷ yield η/π^0 ratios of 0.42 ± 0.08 , 0.56 ± 0.04 , 0.58 ± 0.05 , and 0.55 ± 0.06 at $W = 30.6$, 44.8 , 52.7 , and 62.4 GeV, respectively, for p_\perp in the range $3.0 \leq p_\perp \leq 6.0$ GeV/c. These values are in excellent agreement with our expectations and indicate that perhaps decay mass effects are not important.

5. $\pi N \rightarrow (\pi^+/\pi^-) + X, \pi p \rightarrow (\pi^+/\pi^-) + X$

Having estimated $G_{\pi \rightarrow q}(x)$ in Fig. 4(b) we can predict π^+/π^- ratios with a pion beam. Some of these are shown in Fig. 23. These predictions for smaller x_\perp are not quite on the same footing as those for protons, since they depend on something about the pion structure functions that we do not know, namely, the number of nonvalence quarks. But since for larger x_\perp there should be very few of these, the very large π^+/π^- ratios predicted (Fig. 23) must agree with experiment for our model to be correct. At 90° both beam and target play an important role in determining the flavor of the fragmenting quark and thus $\pi^+ p \rightarrow (\pi^+/\pi^-) X$ is quite different from $\pi^- p \rightarrow (\pi^-/\pi^+) X$. However, owing to the peripheral nature of our quark elastic scattering, in the more forward direction these ratios depend primarily on the quark content of the beam, yielding $\pi^+ p \rightarrow (\pi^+/\pi^-) X \approx \pi^- p \rightarrow (\pi^-/\pi^+) X$. Off a target with equal numbers of protons and neutrons isospin symmetry implies equality of $\pi^+ \rightarrow (\pi^+/\pi^-)$ and $\pi^- \rightarrow (\pi^-/\pi^+)$ at all angles.

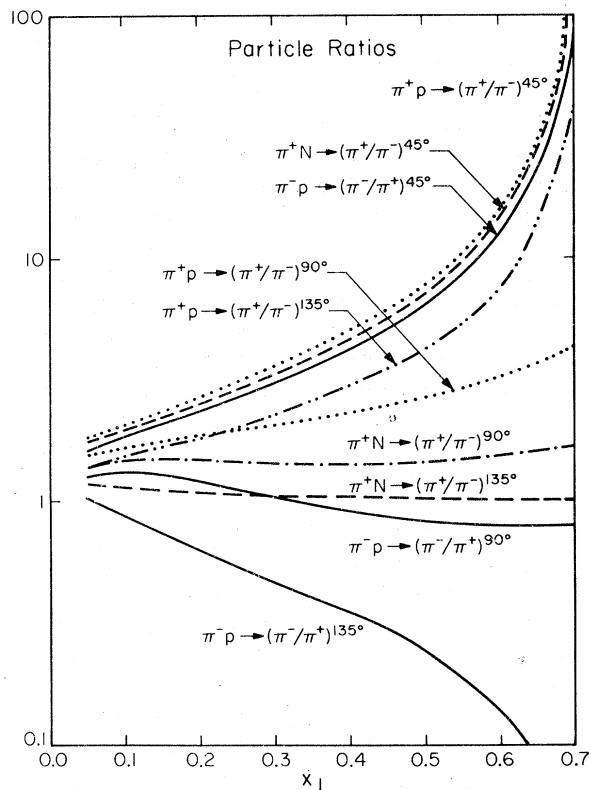


FIG. 23. Predicted ratios from the quark-elastic-scattering model with pion beams: $\pi^\pm p \rightarrow (\pi^\pm/\pi^\mp) + X$, $\pi^\pm N \rightarrow (\pi^\pm/\pi^\mp) + X$ [equals $\pi^\pm N \rightarrow (\pi^\pm/\pi^\mp) + X$] versus x_\perp at $\theta_{c.m.} = 90^\circ$, 45° , and 135° , where $N = (p + n)/2$.

VI. SUMMARY AND CONCLUSIONS

We have investigated the possibility that the rare particles of high transverse momentum ($p_\perp \gtrsim 2$ GeV/c) seen in energetic hadron collisions are cascade fragmentation products from quarks generated in direct elastic quark-quark scattering. This large-angle quark-quark scattering occurs between two quarks, one from the beam hadron and one from the target hadron. The following three ingredients are needed to investigate this model:

- (i) The distribution of quarks within the initial hadrons.
- (ii) The way in which quarks cascade into hadrons. In particular, the probability of finding a meson carrying a certain fraction of the quark's momentum.
- (iii) The differential cross section for quark-quark elastic scattering $d\hat{\sigma}/d\hat{s}, \hat{t}, q_a + q_b \rightarrow q'_a + q'_b$.

In principle the first two are determined by lepton experiments. The structure functions νW_2 for lepton-hadron deep-inelastic scattering de-

termine (i), and the hadron products produced in lepton-hadron scattering, $l + h \rightarrow l' + h' + X$, determine (ii). Then various forms may be tried for the quark-quark collision cross section (iii) to predict the high- p_\perp hadrons in purely hadron collisions. A single form for this agreeing with all experiments (various energies, angles, values of p_\perp , particle ratios coming out, and data for different beams must all agree) would indicate success of the model.

Unfortunately, this ideal scenario must be modified in practice because experiments are not available in sufficient detail or accuracy. At many points we supplement experiment by theoretical arguments.

First the quark distributions (i) in the proton and neutron are fairly well determined by experiment with electrons and neutrinos. However, the behavior near $x=1$ is not known and we add some theoretical considerations from the Drell-Yan relation yielding $xu(x) \sim (1-x)^3$. Furthermore, we use arguments presented in Ref. 1 to conclude that $xd(x) \sim (1-x)^p$, where p is greater than 3. (For simplicity we take $p=4$.) For our purposes data for very small x ($\lesssim 0.1$) are not important, but for completeness we have included this region using Regge arguments and sum rules to help. For the quark distributions in a pion there are, on the other hand, no lepton-scattering data at all. To determine these we have to assume the validity of the model we ultimately wish to test and use data relating the efficacy of π and p beams (on p targets) for producing π^0 [e.g., $\sigma(\pi p \rightarrow \pi^0 X)/\sigma(pp \rightarrow \pi^0 p)$]. Even a crude guess for the distribution function gives a reasonable understanding, while a little more sophisticated function permits a close fit (see Fig. 16). That this may be possible is not trivial curve fitting. For example, a model which assumes that final mesons are produced from quark and antiquark *both* of which must be found in either target or beam predicts a very different ratio indeed, in disagreement with experiment.

Next, for the disintegration properties of the quarks (ii) there are only limited experimental data from $l + h \rightarrow l' + h' + X$ and also from $e^+ e^- \rightarrow$ hadrons. The data from neutrino and electron scattering and $e^+ e^-$ annihilation fortunately all agree, checking our views for lepton reactions. They give us some information on $\omega(z)$, the π/π^+ ratio produced by a u quark, and on the total number of charged pions produced, $D(z) = D_u^{\pi^+}(z) + D_u^{\pi^-}(z)$. To aid in this determination and to go further (e.g., for K^+ , K^- production rates) a large number of theoretical guesses were necessary. They were not all securely based, but one circumstance makes this "guessing of functions"

less of a worry than it might generally be. The hadron experiments, with which we compare our model in this paper, are single-arm experiments triggered by finding one hadron h of large p_\perp . Because all cross sections fall so rapidly (as p_\perp^{-8}) with p_\perp , the quark from which this hadron came had a p_\perp almost as small as possible—only 10 or 20% higher than the p_\perp of the hadron. Therefore the z for which the distribution functions are needed are only in a narrow range near 1, say 0.7 to 1.0. Thus the decays we need here are those in which a quark gives most of its momentum (typically 90%) to one hadron. We assume, theoretically, that if the chance that a hadron h is nearly a pure quark q varies as $(1-x)^p$ for x near 1 [a property of the distribution functions (i)] then the chance that a quark q is nearly a pure hadron varies as $(1-z)^p$ with the same p for z near 1.^{18,19} These ideas are combined with clues from the lepton experiments to determine all these functions, with the exception of one parameter. In the cascade of particles from a quark we assume that new quark pairs are less frequently made if they are strange than if they are nonstrange. This ratio is our parameter and is determined to be 0.5 by looking at K^+ to π^+ production ratios in high- p_\perp hadron collisions.

For the convenience of the reader in reproducing our calculations we have provided computer parametrizations of our quark decay and structure functions. These are found in Tables IV, V, and VI.²⁶

Finally, we turn to item (iii), the dependence of the quark-quark elastic cross section on the invariants \hat{s} and \hat{t} of the quark collisions (or equivalently to the dependence on the energy $\sqrt{\hat{s}}$ and c.m. angle $\hat{\theta}_{c.m.}$). If $d\hat{\sigma}/d\hat{t}$ is a homogeneous function of energy [such as $\hat{s}^{-N}f(\hat{t}/\hat{s})$] then if two hadron collisions at different energy are compared but at the same angles and relative proportion of momenta they should also vary homogeneously with momentum—thus for example for $A + B \rightarrow h + X$ we have

$$E d\sigma/d^3p(s, p_\perp, \theta_{c.m.}) = p_\perp^{-2N} I(x_\perp, \theta_{c.m.}; A + B \rightarrow h). \quad (6.1)$$

Experimental data are not yet even self-consistent, but it looks like these might be correct for $2N$ near 8, and we have assumed it. Naturally then any dependence of cross sections on p_\perp is sensitive to this choice and a fit is more a test of our phenomenological choice for $d\hat{\sigma}/d\hat{t}$ than of our quark-scattering model. On the other hand, we should like to emphasize that there are features of the hadron data that we *must* fit if our model is correct and which are only slightly sensitive

TABLE IV. Computer parametrizations (see Ref. 56) used for the quark distributions within the proton, where each of the functions $G(x)$ are given by $xG(x) = g(x) \sum_{k=0}^N (a_k + \sqrt{x} b_k) C_k(x)$. The Chebyshev polynomials $C_k(x)$ are given by $C_k(x) = \cos[k \cos^{-1}(2x - 1)]$.

$xG(x)$	$xu(x)$	$xd(x)$	$xs(x)$	$x\bar{u}(x)$	$x\bar{d}(x)$	$x\bar{s}(x)$
$g(x)$	$(1-x)^3$	$(1-x)^4$	$(1-x)^8$	$(1-x)^{10}$	$(1-x)^7$	$(1-x)^8$
a_0	161.579	-3.175	0.10	0.17	0.17	0.10
a_1	225.327	-2.937	0.0	0.0	0.0	0.0
a_2	70.699	1.082	0.0	0.0	0.0	0.0
a_3	6.781	0.674	0.0	0.0	0.0	0.0
b_0	-177.909	5.607	0.0	0.0	0.0	0.0
b_1	-230.510	2.634	0.0	0.0	0.0	0.0
b_2	-52.427	-2.288	0.0	0.0	0.0	0.0
b_3	-1.371	-0.247	0.0	0.0	0.0	0.0

to the choice of $d\hat{\sigma}/d\hat{t}$. These constitute a real test of the model. An example, is, at fixed $\theta_{c.m.}$, say 90° , the behavior of $I(x_\perp, \theta_{c.m.}; A + B \rightarrow h)$. In addition, particle and beam ratios (changing A , B , and h) do not depend sensitively on $d\hat{\sigma}/d\hat{t}$. The reason for this is that the exact choice of N only affects slightly the perpendicular momentum of the quark needed to produce a hadron of given x_\perp . It only affects the value of z , which is near 1 [i.e., z is in the neighborhood of $(1 - 1/2N)$], to be a bit closer or further from 1. Not much is altered by this.

The final choice of $f(\hat{t}/\hat{s})$ was determined roughly by comparison to the angular dependence of large- p_\perp production. Again this angular dependence is sensitive to our choice and our fit to data is only curve fitting—we choose finally

$$d\hat{\sigma}/d\hat{t} = 2.3 \times 10^6 \mu b (\text{GeV})^6 / (-\hat{s}\hat{t}^3) \quad (6.2)$$

as a reasonable fit to the data. This gives approximate radial scaling (dependence only on $x_R = x_\perp / \sin\theta_{c.m.}$), but it appears as a numerical accident and not a fundamental principle. This form is to be considered as empirical. We know

of no theory that yields such a form. But again there are many features insensitive to this choice. It affects only slightly the distribution in x_a, x_b , the momenta of the quarks in source and target, needed to produce a given hadron at x_\perp and $\theta_{c.m.}$. The main behavior of $I(x_\perp, \theta_{c.m.}; A + B \rightarrow h)$ as a function of x_\perp , and beam, target and product (A , B , and h) for a given $\theta_{c.m.}$ is insensitive to our choice of (iii) and thus agreement here corresponds to a test of the central ideas of our model [and our choice for items (i) and (ii)]. In Table III we summarize which features are sensitive to our specific choice of function $d\hat{\sigma}/d\hat{t}$ in (iii) and which are insensitive.

We have, in this paper on high- p_\perp single-meson production, not turned up any features of the data which are in such gross disagreement as to exclude the model. (In particular, we see no necessity to include contributions to the single-particle cross section arising from gluons in the incoming particles.) Although some of the tests have been significant, others may simply be the result of judicious choice of functions. It is difficult to give a judgment of the overall significance of our results until we see how future experiments

TABLE V. Computer parametrizations (see Ref. 56) used for the quark distributions within the pion, where each of the functions $G(x)$ is given by $xG(x) = g(x) \sum_{k=0}^N (a_k + \sqrt{x} b_k) C_k(x)$. The Chebyshev polynomials $C_k(x)$ are given in the caption of Table IV.

$xG(x)$	$xu\pi^+(x)$	$x\bar{u}\pi^+(x)$
$g(x)$	1	$(1-x)^5$
a_0	14.758	0.1
a_1	21.171	0.0
a_2	7.491	0.0
a_3	0.996	0.0
a_4	0.013	0.0
b_0	-15.875	0.0
b_1	-22.179	0.0
b_2	-5.753	0.0
b_3	-0.493	0.0
b_4	0.035	0.0

TABLE VI. Computer parametrizations (see Ref. 56) used for the quark decay functions; each of the functions $F(z)$ is given by $zF(z) = f(z) \sum_{k=0}^N a_k C_k(z) + d$. The Chebyshev polynomials $C_k(z)$ are given in the caption of Table IV.

$zF(z)$	$zD(z)$	$zK_u(z)$	$zK_s(z)$	$\omega(z)$
$f(z)$	$(1-z)^2$	$(1-z)^2$	$(1-z)^2$	$(1-z)/(1.2-z)$
a_0	1.198	0.433	0.599	0.685
a_1	0.218	-0.268	-0.144	-0.314
a_2	-0.066	0.109	0.023	0.190
a_3	-0.018	0.002	0.024	-0.065
a_4	0.027	-0.024	-0.004	-0.003
a_5	0.009	0.009	-0.013	0.024
a_6	0.0	0.0	0.0	-0.016
a_7	0.0	0.0	0.0	0.010
d	0.05	0.025	0.05	0.0

compare with our predictions. We have chosen virtually all the input functions, and further calculations that we do should fit data directly without further adjustments. In this paper we have given several such predictions for cross sections, beam ratios, or particle charge ratios, etc., vs x_\perp and $\theta_{\text{c.m.}}$ in regions where data are not yet in (although in many cases they are being measured now). Agreement here would give more objective confidence in the model.

In addition, we are continuing calculations with this model for a wider class of experiments. In particular, we are calculating correlations among particles of large transverse momentum on the opposite (and same) sides of the detected hadron as measured in two-arm experiments. To do this correctly we shall include corrections for the slight transverse momenta of the incoming quarks

as well as momentum components of the hadrons cascading from a quark which are perpendicular to the momentum of that quark. Such effects have very little influence on the predictions of this paper, so we have not included them in our calculations here, but they are crucial in understanding correlation experiments.⁵⁷ Our results will be forthcoming.

ACKNOWLEDGMENTS

We have benefited from the papers by Berman, Bjorken, and Kogut³² and Ellis and Kislinger³³ and acknowledge useful discussions with S. Ellis, G. Farrar, G. Fox, and D. Sivers. In addition, we would especially like to thank D. J. Mellema, who worked closely with us on the pion proton beam ratio analysis.

*Work supported in part by the Energy Research and Development Administration under Contract No. E(11-1)-68.

¹For simplicity and definiteness we assume the collision to be a two-quark to two-quark process. But what we shall do in this paper is to compare quark-quark scattering to lepton-quark scattering and to suppose that (aside from the total cross section) the subsequent events related to the "a" quark in $q_a + q_b \rightarrow q'_a + q'_b$ scattering is the same as what happens in a $q_a + \text{lepton} \rightarrow q'_a + \text{lepton}$ collision (and equally for quark b). It is therefore apparent that what we call an "outgoing quark" in a scattering could be a quark accompanied by a distribution of gluons moving in the same general direction as the quark (analogous to bremsstrahlung photons accompanying an electron). It is only necessary that the complement of gluons be the same as any complement of gluons which may accompany an outgoing quark in a lepton scattering experiment. Again, if the incoming quarks generally radiate "bremsstrahlung" gluons in their incident direction this will not affect our results, provided an equal emission occurs when quarks are scattered by leptons.

²R. P. Feynman, *Photon-Hadron Interactions* (Benjamin, Reading, Mass., 1972).

³Glenys R. Farrar, Nucl. Phys. B77, 429 (1974).

⁴See, for example, V. Barger and R. J. N. Phillips, Nucl. Phys. B73, 269 (1974).

⁵See, for example, B. C. Barish, in *Particles and Fields—1974*, proceedings of the Williamsburg meeting of the Division of Particles and Fields of the American Physical Society, edited by Carl E. Carlson (A.I.P., New York, 1975), p. 1.

⁶S. D. Drell and T.-M. Yan, Phys. Rev. Lett. 24, 181 (1970); G. B. West, *ibid.* 24, 1206 (1970).

⁷R. E. Taylor, in *Proceedings of the 1975 International Symposium on Lepton and Photon Interactions at High Energies, Stanford, California*, edited by W. T. Kirk (SLAC, Stanford, 1976), p. 679.

⁸E. D. Bloom, in *Proceedings of the Sixth International*

Symposium on Electron and Photon Interactions at High Energy, Bonn, Germany, 1973, edited by H. Rollnik and W. Pfeil (North-Holland, Amsterdam, 1974), p. 227.

⁹H. Deden *et al.* (Gargamelle Neutrino Collaboration), Nucl. Phys. B85, 269 (1975).

¹⁰B. P. Roe, in *Proceedings of the 1975 International Symposium on Lepton and Photon Interactions at High Energies, Stanford, California*, edited by W. T. Kirk (SLAC, Stanford, 1976), p. 551.

¹¹H. Harari, Phys. Rev. Lett. 24, 286 (1970); P. V. Landshoff, J. C. Polkinghorne, and R. D. Short, Nucl. Phys. B28, 225 (1971); P. V. Landshoff and J. C. Polkinghorne, *ibid.* B28, 240 (1971); J. Kuti and V. Weisskopf, Phys. Rev. D 4, 3418 (1971); J. D. Bjorken, invited talk at the International Conference on Duality and Symmetry in Hadron Physics, Tel Aviv, 1971 (unpublished).

¹²The ratio of $\frac{2}{3}$ for the size of the $1/\sqrt{\nu}$ term in the γ -n and γ -p total cross sections implies that b/b' should be 2. Our fit gave a ratio close to this value ($b/b' = 2.16$).

¹³Recent data on $\nu W_2^{10}(x)$ at large Q^2 in fact show no dip at small x ; H. L. Anderson *et al.* (Chicago-Harvard-Illinois-Oxford collaboration), Phys. Rev. Lett. 37, 4 (1976); 37, 1034 (1976) (E).

¹⁴This fact was pointed out to us by F. Ravndal. See also P. V. Landshoff and J. C. Polkinghorne, Nucl. Phys. B53, 473 (1973).

¹⁵There is an alternative theoretical viewpoint for understanding these form factors that yields $\nu W_2^{10}(x) \sim (1-x)^2 + C/Q^2$ as $x \rightarrow 1$. See, for example, Glenys R. Farrar and Darrell R. Jackson, Phys. Rev. Lett. 35, 1416 (1975).

¹⁶J. D. Bjorken, informal remarks at the New York Academy of Science Conference on Recent Advances in High Energy Physics, New York, 1973 (unpublished).

¹⁷A. Casher, J. Kogut, and Leonard Susskind, Phys. Rev. Lett. 31, 793 (1973).

¹⁸See the review article, by J. D. Sullivan, presented at

- the SLAC Topical Conference on Deep Inelastic Electroporation, 1973, Report No. ILL-(th)-73-11 (unpublished).
- ¹⁹S. D. Drell, D. J. Levy, and T.-M. Yan, Phys. Rev. D 1, 1617 (1972); P. V. Landshoff and J. C. Polkinghorne, *ibid.* 6, 3708 (1972); R. Gatto, P. Menotti, and I. Vendramin, *ibid.* 7, 2524 (1973). For a recent model in which the coefficients c and c' are not equal see Martin B. Einhorn, University of Michigan Report No. UMHE76-36, 1976 (unpublished).
- ²⁰R. N. Chan and E. W. Colglazier, Phys. Rev. D 9, 2658 (1974); Glennys R. Farrar and Jonathan L. Rosner, *ibid.* 10, 2226 (1974).
- ²¹M. Gronau, F. Ravndal, and Y. Zarmi, Nucl. Phys. B51, 611 (1973).
- ²²M. Haguenauer, in *Proceedings of the XVII International Conference on High Energy Physics, London, 1974*, edited by J. R. Smith (Rutherford Laboratory, Chilton, Didcot, Berkshire, England, 1974), p. IV-95.
- ²³Jean Cleymans and Rudolf Rodenberg, Phys. Rev. D 9, 155 (1974).
- ²⁴C. H. Albright and J. Cleymans, Nucl. Phys. B76, 48 (1974).
- ²⁵J. Cleymans and L. M. Sehgal, Nucl. Phys. B61, 479 (1973).
- ²⁶The open triangles in Fig. 5(a) are the determination of $1/\omega(z)$ by L. Sehgal (Ref. 28) using the eN data of Ref. 29.
- ²⁷J. T. Dakin and G. J. Feldman, Phys. Rev. D 8, 2862 (1973).
- ²⁸L. M. Sehgal, Nucl. Phys. B90, 471 (1975).
- ²⁹J. T. Dakin, G. J. Feldman, F. Martin, M. L. Perl, and W. T. Toner, Phys. Rev. D 10, 1401 (1974).
- ³⁰F. J. Gilman, in *Proceedings of the 1975 International Symposium on Lepton and Photon Interactions at High Energies, Stanford, California*, edited by W. T. Kirk (SLAC, Stanford, 1976), p. 131.
- ³¹For a review, see D. Sivers, S. J. Brodsky, and R. Blankenbecler, Phys. Rep. 23C, 1 (1976).
- ³²J. D. Bjorken, Phys. Rev. D 8, 4078 (1973); S. M. Berman, J. D. Bjorken, and J. B. Kogut, *ibid.* 4, 3388 (1971).
- ³³S. D. Ellis and M. B. Kislinger, Phys. Rev. D 9, 2027 (1974); S. D. Ellis, in *Proceedings of the XVII International Conference on High Energy Physics, London, 1974*, edited by J. R. Smith (Rutherford Laboratory, Chilton, Didcot, Berkshire, England, 1974), p. V-23; S. D. Ellis and R. Thun, in *High Energy Hadronic Interactions*, proceedings of the IX Rencontre de Moriond, Méribel-les-Allues, France, 1974, edited by J. Tran Thanh Van (CNRS, Paris, 1974); S. D. Ellis, M. Jacob, and P. V. Landshoff, Nucl. Phys. B108, 93 (1976).
- ³⁴W. Furmanski and J. Wosiek, Jagellonian University Report No. TPJU-8/76, 1976 (unpublished); W. Furmanski and J. Wosiek, Jagellonian University Report No. TPJU-7/76, 1976 (unpublished).
- ³⁵R. Blankenbecler, S. J. Brodsky, and J. F. Gunion, Phys. Rev. 106, 2652 (1972); Phys. Lett. 42B, 461 (1973); R. Blankenbecler, S. J. Brodsky, Phys. Rev. D 10, 2973 (1974); J. F. Gunion, *ibid.* 10, 242 (1974); R. Blankenbecler, S. J. Brodsky, and J. Gunion, *ibid.* 12, 3469 (1975); Risto O. Raitio and Gordon A. Ringland, *ibid.* 14, 2291 (1976); Risto Raitio, University of Wisconsin Report No. COO-545, 1976 (unpublished).
- ³⁶P. V. Landshoff, J. C. Polkinghorne, Phys. Rev. D 8, 927 (1973); 8, 4157 (1973); 10, 891 (1974).
- ³⁷For colorless quarks of the same flavor exchanging one vector gluon (as for e^-e^- scattering in electrodynamics) the scattering goes as $(\hat{s}^2 + \hat{t}^2)/(\hat{s}^2 \hat{t}^2 + (\hat{s}^2 + \hat{t}^2)/\hat{s}^2 \hat{u}^2 + 2/\hat{t}\hat{u})$, the last term representing interference. This interference is relatively largest at 90° , where it increases the scattering by 80%. For colored quarks exchanging singlet gluons (i.e., not exchanging color) the interference is reduced by a factor of 3 since like colored quarks meet in only $\frac{1}{3}$ of the collisions. For octet-vector-gluon exchange a short calculation shows the interference term is changed in sign and reduced by the factor 3 (i.e., it is $-2/3\hat{t}\hat{u}$). The observed p_\perp^{-3} behavior of the data implies that none of these mechanisms hold; possibly several gluons are exchanged, etc. Thus we can estimate neither the sign nor magnitude of the interference term at this time.
- ³⁸K. Kauffmann suggested (private communication) the possibility that the quark-quark force would be via vector particles of momentum k with propagator $1/k^4$ because it gives a confining potential rising linearly with distance and soft forces at short distances. This corresponds to form (4.8a). The factor $(\hat{s}^2 + \hat{t}^2)/\hat{s}^2$ is roughly equivalent to $(\hat{s}/-\hat{t})^{0.25}$ for $\theta_{c.m.}$ from 45° to 135° .
- ³⁹B. Alper *et al.* (British-Scandinavian collaboration), Nucl. Phys. B100, 237 (1975).
- ⁴⁰M. B. Albrow *et al.* (CHLM collaboration), Nucl. Phys. B73, 40 (1974).
- ⁴¹F. E. Taylor *et al.*, Phys. Rev. D 14, 1217 (1976). Actually these authors define $x_R = E_R/E_{max}$, where E_R is the energy of the detected hadron. Since we are dealing with pions we neglect the difference between energy and momentum.
- ⁴²We have investigated the behavior of existing data on $p\bar{p} \rightarrow \pi^+X$ versus W at fixed x_R and believe that the data show a slight rise as W increases from Fermilab to ISR energies. This is a difficult analysis because there is only a small region of x_R where data from these two energy domains overlap. Nevertheless, it is clear that the cross section is not falling at fixed x_R versus W which disfavors the extremely nonperipheral form (4.8d) for $d\sigma/d\hat{t}$.
- ⁴³S. Brodsky and G. Farrar, Phys. Rev. Lett. 31, 1153 (1973); Phys. Rev. D 11, 1309 (1975).
- ⁴⁴H. D. Politzer, Phys. Rep. 14C, 129 (1974).
- ⁴⁵A. De Rújula, H. Georgi, and H. D. Politzer, Ann. Phys. (N.Y.) 103, 315 (1977).
- ⁴⁶K. Eggert *et al.* (ACHM collaboration), Nucl. Phys. B98, 49 (1975).
- ⁴⁷F. W. Busser *et al.* (CCRS collaboration), Nucl. Phys. B106, 1 (1976).
- ⁴⁸We have assumed that $\omega(x) \sim (1-x)^3$ for $x \geq 0.8$ [(2.5a)]. Recent data on eN scattering indicate that $\nu W_2(x)$ may fall off more rapidly, perhaps as $(1-x)^4$ (see, for example Ref. 6). If true, this would cause our predicted $I(x_\perp, \theta)$ function in Fig. 14 and Fig. 15 to fall off faster in the large x_\perp region ($x_\perp \gtrsim 0.6$ for $\theta=90^\circ$) yielding an asymptotic form $(1-x_\perp)^{10}$ rather than the $(1-x_\perp)^8$ now predicted. There is insufficient data on $p\bar{p} \rightarrow \pi^+X$ for $x_\perp \geq 0.6$ to test these asymptotic forms.
- ⁴⁹G. Donaldson, H. Gordon, K.-W. Lai, I. Stumer, A. Barnes, D. J. Mellem, A. Tollestrup, R. Walker, O. Dahl, R. A. Johnson, A. Ogawa, M. Pripstein, and

⁵¹S. Shannon, Phys. Rev. Lett. 36, 1110 (1976).

⁵⁰As discussed in Sec. IV A in the absence of interference terms our model predicts $\sigma(\pi^+ p \rightarrow \pi^0 X) = \sigma(\pi^- p \rightarrow \pi^0 X)$.

⁵¹Clearly this estimate depends strongly on the precise behavior of the antiquark distributions within the proton and upon the quark distributions within the pion, about which little is known. Other choices for these quantities will lead to somewhat different pion to proton beam ratios. See, for example, B. L. Combridge, Phys. Lett. 62B, 222 (1976).

⁵²The Fermilab data of Cronin *et al.* (see Fig. 13 caption) are taken off heavy nuclei, and an attempt is made to extrapolate these results to an "effective" nucleon. Since these large p_\perp cross sections are not strictly proportional to the number of nucleons, A (for example, some vary as $A^{1.3}$) and there is, as yet, no detailed theory for the actual A dependences observed, these extrapolations are unreliable, and any data obtained in this manner must be viewed with caution.

⁵³During the writing of this paper we have learned (H. Frisch, private communication) that recent data taken off protons at Fermilab do show a substantial increase in the ratio $p\bar{p} \rightarrow (\pi^+/\pi^-) + X$ as x_\perp becomes large. This ratio is greater than 2 at $x_\perp \approx 0.5$, in ex-

cellent agreement with our predictions.

⁵⁴The limiting behavior of $u(x)/d(x)$ for large x is of theoretical interest (we have assumed it goes to infinity) but is difficult to determine by lepton experiments.

Hadron experiments may permit us to determine it because the very high π^+/π^- ratios predicted at large x_R in Fig. 21 are a reflection of the large $u(x)/d(x)$ ratio that we have assumed for large x . If, in fact, $u(x)/d(x)$ does not go to infinity but to some constant, say 5, the predicted $p\bar{p} \rightarrow (\pi^+/\pi^-) + X$ ratio would begin to deviate from Fig. 21 for $x_R \gtrsim 0.6$ and approach 5 as $x_R \rightarrow 1$.

⁵⁵See, for example, R. G. Moorhouse, invited talk given at the Triangle Conference, Slovakia, 1975, CERN Report No. TH.2103 (unpublished).

⁵⁶The quark decay functions $D_q^h(z)$ and quark distributions $G_{h \rightarrow q}(x)$ originally used in our calculations were combinations of analytic functions and hand-drawn curves (which were digitized and interpolated by the computer). For the convenience of the reader in reproducing our results we have provided the parametrization given in Tables IV, V, and VI. These parametrizations are fits to our, in some cases, hand-drawn curves and this is the reason for their odd appearance.

⁵⁷R. Baier, J. Cleymans, K. Kinoshita, and B. Petersson, Nucl. Phys. B118, 139 (1977).